AGU PUBLICATIONS

Water Resources Research

RESEARCH ARTICLE
10.1002/2015WR017185

Key Points:
- Three-phase oil relative permeability depends on saturation path
- Residual saturation is the key factor in modeling relative permeability
- Residual oil saturation is a function of water saturation

Correspondence to:
A. Kianinejad,
kianinejad.amir@utexas.edu

Citation:
Kianinejad, A., X. Chen, and D. A. DiCarlo (2015), The effect of saturation path on three-phase relative permeability, *Water Resour. Res.*, *51*, 9141–9164, doi:10.1002/2015WR017185.

Received 3 MAR 2015
Accepted 27 OCT 2015
Accepted article online 30 OCT 2015
Published online 22 NOV 2015

© 2015. American Geophysical Union. All Rights Reserved.

The effect of saturation path on three-phase relative permeability

Amir Kianinejad[1], Xiongyu Chen[1], and David A. DiCarlo[1]

[1]Department of Petroleum and Geosystems Engineering, University of Texas at Austin, Austin, Texas, USA

Abstract Simulation and fluid flow prediction of many petroleum-enhanced oil recovery methods as well as environmental processes such as carbon dioxide (CO_2) geological storage or underground water resources remediation requires accurate modeling and determination of relative permeability under different saturation histories. Based on this critical need, several three-phase relative permeability models were developed to predict relative permeability; however, for practical purposes most of them require a variety of parameters introducing undesired complexity to the models. In this work, we attempt to find out if there is a simpler way to express this functionality. To do so, we experimentally measure three-phase, water/oil/gas, relative permeability in a 1 m long water-wet sand pack, under several saturation flow paths to cover the entire three-phase saturation space. We obtain the in situ saturations along the sand pack using a CT scanner and then determine the relative permeabilities of liquid phases directly from the measured in situ saturations using an unsteady state method. The measured data show that at a specific saturation, the oil relative permeability varies significantly (up to two orders of magnitude), depending on the path through saturation space. The three-phase relative permeability data are modeled using standard relative permeability models, Corey-type, and Saturation Weighted Interpolation (SWI). Our measured data suggest that three-phase oil relative permeability in water-wet media is only a function of its own saturation if the residual oil saturation is treated as a function of two saturations. We determine that residual saturation is the key parameter in modeling three-phase relative permeability (effect of saturation history).

1. Introduction

Multiphase flow occurs in many petroleum reservoir processes including enhanced oil recovery methods and during environmental processes such as CO_2 geological storage or infiltration and migration of nonaqueous phase liquid (NAPL) pollutants during or after rainfalls due to the leakage from underground petroleum hydrocarbon and industrial hazardous chemical storage facilities [*Huyakorn et al.*, 1994; *Pandy et al.*, 1995; *Moortgat et al.*, 2011; *Mohsenzadeh et al.*, 2011; *Hosseini et al.*, 2013; *Aminzadeh-goharrizi et al.*, 2012; *Sun et al.*, 2014]. In order to model multiphase flow, accurate determination of relative permeabilities are required as one of the essential input parameters [*Juanes et al.*, 2006; *Rezaveisi et al.*, 2010; *Zuo et al.*, 2012; *Krevor et al.*, 2012; *Mohsenzadeh et al.*, 2012; *Pini and Benson*, 2013; *Reynolds et al.*, 2014; *Chen et al.*, 2014; *Kuo and Benson*, 2015]. In two-phase systems, it is straightforward but not simple to measure relative permeabilities since there are only two possible saturation paths for the flow; if one phase saturation decreases, the other phase saturation must increase. This situation becomes much more complicated in three-phase systems, because two phase saturations can change independently, resulting in an infinite number of saturation paths [*Carlson*, 1981; *Blunt*, 2000; *Shahrokhi et al.*, 2014; *Akbarabadi and Piri*, 2013; *Alizadeh and Piri*, 2014]. In addition, experimental measurements have shown that, in three-phase systems, the relative permeability of nonwetting phases tend to depend on the saturation history, and are a function of more than one phase saturation [*Holmgren and Morse*, 1951; *Oak*, 1990; *Oak et al.*, 1990; *Skauge and Larsen*, 1994; *Dehghanpour et al.*, 2010; *Fatemi et al.*, 2012; *Kianinejad et al.*, 2014]. However, there exists a limited number of experimental three-phase relative permeability measurements, which are sometimes contradictory to each other, making a physical understanding of this functionality difficult [*Delshad and Pope;* 1989; *Oak et al.*, 1990; *Skauge and Larsen*, 1994; *Eleri et al.*, 1995; *Alizadeh and Piri*, 2014]. In addition, most of these experimental data are limited to a few number of saturation paths in three-phase saturation space [*Holmgren and Morse*, 1951; *Saraf et al.*, 1982; *Schneider and Owens*, 1970; *Oak*, 1990; *Skauge and Larsen*, 1994; *Eleri et al.*, 1995; *Fatemi et al.*, 2012; *Dehghanpour and DiCarlo*, 2013a]. Consequently, any additional measurements of three-phase relative permeability over a larger saturation space and methods to obtain large quantities of three-phase data are necessary to obtain a better understanding of this phenomenon.

Several authors measured three-phase relative permeabilities under various conditions. Oak and coworkers [*Oak*, 1990, 1991; *Oak et al*., 1990] performed the most extensive steady state three-phase measurements. They found that in water-wet media, three-phase water relative permeability is almost independent of saturation history, while the three-phase oil relative permeability is a function of saturation history, and the saturation of all existing phases.

Skauge and Larsen [*Skauge and Larsen*, 1994; *Eleri et al*., 1995] conducted several steady state and unsteady state experimental measurements on relative permeabilities during water alternating gas (WAG) injection method. In agreement with Oak and coworkers [*Oak*, 1990, 1991; *Oak et al*., 1990], they concluded that, the three-phase relative permeability of the wetting phase is only a function of its own saturation and independent of saturation history; with the relative permeability of the intermediate-wetting phase is a function of more than one phase saturation and saturation history.

Sahni et al. [1998] measured three-phase relative permeabilities during gravity drainage experiments by measuring in situ saturations using CT scanning. They observed that, at low saturations the three-phase oil and water relative permeabilities are only a function of their own saturations for particular paths through saturation space. *DiCarlo et al*. [2000a, 2000b] extended the work to other wettability conditions. They observed that, in spreading systems, the three-phase oil relative permeability behavior at low saturations is different from high saturations, a characteristic of oil layer drainage mechanism. *Dehghanpour et al*. [2010, 2011; *Dehghanpour and DiCarlo*, 2013a] used the same methodology to measure two and three-phase relative permeabilities. They found a pronounced change in three-phase oil relative permeability depending on the initial condition of the experiments.

Sohrabi and coworkers conducted a series of experimental studies on WAG injection at near miscible conditions, using unsteady state method. They reported an irreversible hysteresis in three-phase relative permeability [*Fatemi et al*., 2011; *Fatemi et al*., 2012].

Recently, *Alizadeh and Piri* [2014] conducted steady state three-phase relative permeability measurements along various saturation paths to investigate the effect of saturation history on three-phase relative permeability. They observed that the oil relative permeability is a function of all the existing phases' saturations, and independent of saturation history. Their results for the oil phase, which is intermediate-wetting phase, differs from the observations of others [*Oak*, 1990, 1991; *Skauge and Larsen*, 1994; *Eleri et al*., 1995] in terms of dependency on saturation history.

There exist two broad categories for measuring relative permeability as, steady state and unsteady state methods for special core analysis [*Jones and Roszelle*, 1978; *Fassihi and Potter*, 2009]. The steady state method is a straightforward method to measure two-phase relative permeabilities. However, for three-phase measurements, this method is time consuming, expensive, requires large amount of fluids, and provides a limited number of points on the relative permeability curves [*Honarpour and Mahmood*, 1988]. On the other hand, unsteady state measurements are faster, and cheaper to conduct; but sometimes require interpretations and assumptions. For instance, a well-known unsteady state procedure to calculate relative permeability is the Welge-JBN and its modifications [*Johnson et al*., 1959; *Sarem*, 1966; *Saraf et al*., 1982]. However, *Mohanty and Miller* [1991] showed that the assumptions made in the JBN method [*Johnson et al*., 1959] do not capture the exact processes occurring during displacement measurements. A different approach to measure relative permeability using unsteady state method is history matching the in situ saturations measured during displacement experiments [*Vizika and Lombard*, 1996]. However, the relative permeabilities obtained from this method are not unique due to the nature of inverse problem solving, and the calculations are sensitive to heterogeneity and capillary pressures [*Siddiqui et al*., 1996; *Vizika and Lombard*, 1996; *Akin and Demiral*, 1997; *Sahni et al*., 1998]. In this work, we use a similar approach to measure the relative permeabilities during unsteady state displacements in terms of measuring in situ saturations along the porous media at different times. However, we show under certain conditions that the relative permeabilities can be calculated directly from the measured saturation profiles.

It has been shown that the performance of existing three-phase models against the experimental data are not satisfactory [*Delshad and Pope*, 1989; *Blunt*, 2000; *Spiteri et al*., 2008; *Shahverdi et al*., 2011]. Consequently, several authors developed new models to account for saturation path and hysteresis effects [*Larsen and Skauge*, 1995; *Jerauld*, 1997; *Blunt*, 2000; *Spiteri et al*., 2008; *Shahverdi and Sohrabi*, 2012; *Shahverdi and Sohrabi*, 2013; *Beygi et al*., 2015]. However, these models require additional procedures to consider saturation paths variations (hysteresis), for instance gas trapping, introducing complexity for practical use purposes by requiring calculation of several parameters [*Land*, 1968; *Carlson*, 1981; *Jerauld*, 1997; *Larsen and Skauge*, 1998; *Blunt*, 2000; *Spiteri et al*., 2008; *Beygi et al*., 2015].

In this work, we attempt to find a simpler way with fewer parameters to express the functionality of three-phase relative permeability. To achieve this goal, we first obtain three-phase, water/oil/gas, relative permeabilities along several saturation paths in order to extend our three-phase measurements over the entire three-phase saturation space. We then show how this extension provides us a better understanding of three-phase flow over the entire saturation space.

We extend the unsteady state, gravity drainage method used by *Sahni et al*. [1998]; *DiCarlo et al*. [2000a, 2000b]; *Dehghanpour et al*. [2010]; and *Kianinejad et al*. [2014] to overcome the previous limitations and extend the measurements over a larger saturation space. We first present the two phase measurements using this extended method, and compare it with the previous conventional method. We then explain how these two-phase measurements validate our new methodology for relative permeability measurements. In the next step, we present three-phase relative permeability measurements for a series of three-phase experiments covering the entire three-phase saturation space to quantify the effect of saturation path (saturation history) on three-phase relative permeability. Finally, we test the performance of standard models against our set of experimental data.

2. Materials and Methods

2.1. Porous Media

A 3 feet long column of water-wet sand pack was used as the porous media. The sand was packed into a rubber sleeve column with an inner diameter of 7.5 cm. The same sand particles were used as that of *Dehghanpour and DiCarlo* [2013b] used, with the average sand grain diameter of 0.25 mm (refer to *Dehghanpour and DiCarlo* [2013b] for details on sand particle-size distribution). A confining pressure of 50 psi (345 kPa) was provided by water to stabilize the pack and prevent flow near the edge. The porosity and permeability of the sand pack were measured to be 0.365 and 13 darcy (1.3×10^{-11} m^2), respectively. The porosity was determined by measuring the maximum amount of water possible to inject to the dry, vacuumed column, and the permeability was measured using the single-phase flow water injection. Syringe pumps were used to displace and inject the working fluids.

2.2. Calibration and Fluids

Three calibration scans were required to measure three-phase saturation. The column was calibrated while it was dry and 100% saturated with gas, 100% saturated with brine, and finally 100% saturated with oil phase. The oil calibration was performed by flushing the drained column after two-phase, water/gas experiments with one pore volume of isopropyl alcohol. Isopropyl alcohol is miscible with the oil phase and the brine phase, and the alcohol was injected from the bottom while vacuuming from the top to dissolve the residual water. Then, two pore volumes of oil were injected from the top to remove all the alcohol by maintaining a gravity-stable, miscible displacement. This achieved a 100% oil saturated sand pack column without repacking the column to keep the porous media the same for all the experiments. Aqueous solution of 10 wt % NaBr was used as the brine, n-octane as the oil phase, and air as the gas phase. The injected gas was first bubbled through a column of water and oil in order to saturate the vapor with these fluids before injecting to the porous media. This presaturation eliminates the effect of evaporation of fluids on the measured saturation profiles inside the porous media.

2.3. In Situ Saturation Measurement

The saturations along the column were obtained using a dual energy CT scanning technique. A modified medical CT scanner was used to scan the column during the drainage experiments. For three-phase systems, the column was scanned twice at two energy levels (100 and 140 kV), in 3 cm intervals, and from the top to the bottom while moving the column by a vertical positioning system in order to measure the fluid saturations along the sand pack column. Scanning the column at two energy levels provided us two independent linear equations. Given that the summation of existing fluid saturations equals one, these equations were simultaneously solved and the in situ saturations along the column was calculated at different times. It should be mentioned that calculating the in situ saturations for two-phase systems required scanning the column at only one energy level. The measured saturations during three-phase experiments in our sand pack are biased by 0.003 saturation units, while this value is even smaller in two-phase systems [*Dehghanpour*, 2011]. In all experiments, the column was vertically oriented and scanned at different times to measure the in situ fluid saturations. The results of the experiments are $S(z,t)$ for each phase, at time

intervals of 5 min or less. Figure 1 shows the saturation profiles measured during the two-phase (water/gas) experiments as a function of space and time.

2.4. Overview of Obtaining Relative Permeability From Saturation Versus Space and Time

From these measurements, we now obtain relative permeability of the liquid phase. The method is outlined in detail below, and requires the following assumptions which are met in our experiments:

1. One-dimensional flow in vertical direction
2. Negligible gas potential gradient due to low viscosity and flow rate of gas
3. Liquids drain under their own gravitational gradient only

For each phase, we use the following method to obtain relative permeabilities. Assuming one-dimensional flow in the vertical (z) direction and incompressible fluids, we start with the Darcy-Buckingham equation,

$$u_i = -\frac{kk_{ri}}{\mu_i}\frac{\Delta\Phi_i}{\Delta z} = -\frac{kk_{ri}}{\mu_i}\left(\frac{\Delta P_i}{\Delta z} - \rho_i g\right) \tag{1}$$

where u is the flux, k is the absolute permeability, k_r is the relative permeability, μ is the viscosity,Φ is the potential, P is the pressure, ρ is the density, g is the acceleration of gravity, and z is the position along the porous media being positive downward. Subscript i denotes the liquid phase, i.e., water or oil. Hence the relative permeability at each point and time (t) is given by

$$k_{ri}(z,t) = \frac{-u_i(z,t)\mu_i}{k\left(\frac{\Delta P_i(z,t)}{\Delta z} - \rho_i g\right)} \tag{2}$$

To use this equation to calculate relative permeabilities, one needs to know $u_i(z,t)$ and $\frac{\Delta P_i(z,t)}{\Delta z}$. One also needs $S_i(z,t)$ to match with the obtained $k_{ri}(z,t)$ to get a relative permeability curve.

In the following, we show how under certain conditions, measurements of $S_i(z,t)$ are enough to obtain $u_i(z,t)$ and $\frac{\Delta P_i(z,t)}{\Delta z}$. We then detail how we can extend the range on where these conditions are met during our experiments.

We obtain the flux $u_i(z,t)$ of each phase from our measurements of $S_i(z,t)$ and the boundary conditions. Material balance gives us

$$u_i(z*, t_{j+1/2}) = \frac{\sum_{z=0}^{z*}\left(\left[S_i(z,t_{j+1}) - S_i(z,t_j)\right]\phi\Delta z\right)}{t_{j+1} - t_j} + u_{i_{ext}} \tag{3}$$

where z is the distance from the top of the sand pack column, ϕ is the porosity, and $u_{i_{ext}}$ is the external fluid influx of each phase. Subscript j denotes the time step of each saturation profile.

The other unknown quantity needed is $\frac{\Delta P_i}{\Delta z}$. This is much harder to obtain; instead we design the experiments to obtain large spatial and temporal regions where

$$\left|\frac{\Delta P_i}{\Delta z}\right| < 0.1\rho_i g \tag{4}$$

If we are within one of these regions, we can use the approximation $\rho_i g + \frac{\Delta P_i}{\Delta z} \cong \rho_i g$ and obtain relative permeabilities within 10% (see equation (2)).

We do not have direct pressure measurements; instead we use the saturation profile and the known P-S curve for the media. When the gas flow rate is small compared to the permeability, $q_g \ll \frac{k_g}{\mu_g}$, once the main drainage front moves through, $P_g(z) = const.$ due to its low viscosity. Thus

$$\frac{\Delta P_i}{\Delta z} = -\frac{\Delta P_{c_{gi}}}{\Delta z} = -\left(\frac{dP_{c_{gi}}}{dS_i}\right)\frac{\Delta S_i}{\Delta z} \tag{5}$$

Thus the condition for the ignorance of $\frac{\Delta P_i}{\Delta z}$ becomes

$$\left|\frac{\Delta S_i}{\Delta z}\right| < 0.1\rho g\left(\frac{dP_{c_{gi}}}{dS_i}\right)^{-1} \tag{6}$$

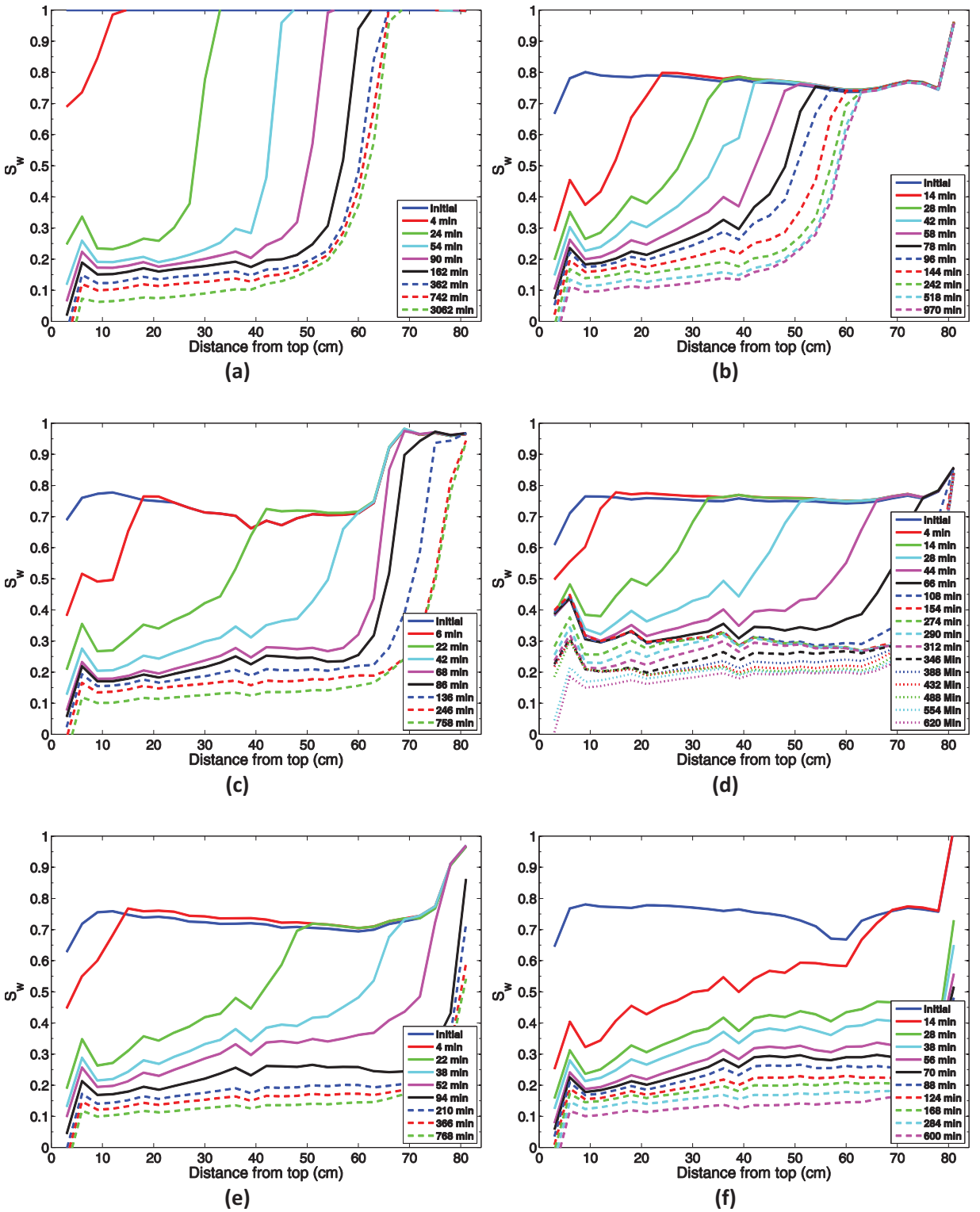

Figure 1. Water saturation profile along the sand pack column at different times during the two-phase (water/gas) experiments: (a) Test 1, (b) Test 2, (c) Test 3, (d) Test 4, (e) Test 5, and (f) Test 6.

Looking at the profiles in Figure 1, e.g., Figure 1a, we can see that at long times ($t > 45$ min) and in the spatial region between $z > 10$cm and $z < 50$cm, $\frac{\Delta S_w}{\Delta z} < 0.003$ cm^{-1}. Moreover, the last (t = 3062 min) saturation profile in Figure 1a (dashed green curve) we use as the defacto capillary pressure curve ($P_c - S_w$) of the

porous medium, as this is the closest to capillary-gravity equilibrium. By comparison, $\rho g\left(\frac{dP_c}{dS_w}\right)^{-1} < 0.075\text{cm}^{-1}$, thus this condition is met in this region.

Importantly, the condition is not met for

1. Early time frontal shocks: when the main wetting front moves through, $\frac{\Delta S_i}{\Delta z}$ is large because of a shock at the front. Thus the only saturations where the criteria can be met is $10 < z < 40$cmand $S_i < S_{Front}$.
2. Outlet: at the outlet, for gravity drainage $\frac{dP}{dS_i}\frac{dS_i}{dz} \approx \rho g$ when $P_c \leq P_c^{entry}$ or in other words for
$$z > z^{End} - \frac{\alpha P_c^{Entry}}{\rho g} \tag{7}$$
where α is a numerical constant which grows slightly with time.
3. Inlet: for the inlet, the effect is more subtle. The capillary effects caused by the discontinuity in flux gives that the region $z < 10$cm does not meet the criteria. It is evident that long columns are needed to obtain as many points away from the end effects.

If we have a region in the column where the above mentioned conditions are met ($\frac{dP_c}{dS_i}\frac{\Delta S_i}{\Delta z} \ll \rho_i g$), the capillary term will be negligible and thus the relative permeability can be found at each measurement point in space and time using the reduced form of equation (2)

$$k_{ri} = \frac{u_i \mu_i}{k \rho_i g} \tag{8}$$

where u_i can be found from two successive saturation profiles.

This method has been used for free gravity drainage in *DiCarlo et al*. [2000a, 2000b]; *Dehghanpour et al*. [2010]; and *Dehghanpour and DiCarlo* [2013a]. In these works, the region where the criteria $\frac{dP_c}{dS_i}\frac{\Delta S_i}{\Delta z} \ll \rho_i g$ was held was typically for $z > 15$cm and $z < 60$cm in a 90cm long sand pack, for times $t > 1$ h. From this, relative permeabilities were calculated only for $S < 0.3$ due to the fast saturation drop across the moving front at early times. As a result, relative permeabilities at larger saturations could not be obtained because the criteria were not met. Here we use methods to increase this region including: different initial states, adding forced gas injection, and also using water and oil injection. In this manner, we overcome the limitation of previous measurements, namely extending relative permeability measurements over a larger phase space, and covering the entire three-phase space through the control of saturation path.

We note that this method is not applicable to two-phase oil/water systems since the criteria detailed above will not be met due to the comparable viscosity and density of water and oil.

2.5. Experimental Procedure

In the subsequent sections, we use two-phase experiments to first show how using the above mentioned techniques expand the spatial region and the saturation phase space for the calculation of relative permeabilities, and then extend the method to three-phase systems.

2.5.1. Two-Phase Experiments

2.5.1.1. Saturation Data

Six gas/water drainage experiments were conducted to verify the experimental methodology and measure two-phase water relative permeability. For the two-phase measurements, the column was set at a different initial condition for each experiment. Figure 1 shows the water saturation profiles along the porous media at different times during the two-phase experiments. Figure 1a shows the water saturation profile for the primary free gravity drainage experiment, Test 1. Here, the column was at the initial condition of fully water saturated. The top and the bottom of the column were then opened to the atmosphere and allowed to drain by gravity. This test was conducted in the conventional method, previously used by others [*DiCarlo et al*., 2000a, 2000b; *Dehghanpour et al*., 2010; *Dehghanpour and DiCarlo*, 2013a]. As one can see in Figure 1a, the water saturation drops to $S_w < 0.3$ behind a spatially abrupt front. The front stops at z=60cm, due to capillary effects. Consequently, per the discussion from last section, in this experiment only the interval of z=10cm to z=40cm of the column can be used for relative permeability calculation, after passage of the front, meaning only saturations below 0.3 are available for relative permeability calculations.

Table 1. Two-Phase (Water/Gas) Experiments With Different Initial and Conducting Conditions

Test	Type	Gas Injection Pressure (kPa)	Water Injection Rate (cc/min)	Injection Period (min)
1	Primary free gravity drainage			
2	Secondary free gravity drainage			
3	Secondary drainage	1.9		
4	Secondary drainage	2	2.2	240
			0.5	240
			0	140
5	Secondary drainage	2.2		
6	Secondary drainage	2.8		

For Tests 2– 6, the initial state of the column was water saturated with some trapped gas in the system. To achieve this initial state, the column was flooded with water after each drainage experiment without applying vacuum.

Figure 1b shows the water saturation profile during the secondary free gravity drainage experiment, Test 2. In Test 2, the top and the bottom of the column is opened to the atmosphere to drain by gravity. The same as Test 1, this test was conducted in the conventional method. Figure 1b indicates that, while the capillary end effect extension is the same as primary free gravity drainage experiment (see Figure 1a), a larger saturation space is available for relative permeability calculations, as the saturation profiles are more smeared compared to primary free gravity drainage experiment (see Figure 1a). Here $\frac{dS_w}{dz} < 0.0025\,\mathrm{cm}^{-1} < 0.1|\rho g\left(\frac{dP_c}{dS_w}\right)^{-1}|$ for $S_w < 0.45$ in the spatial region between $z > 10$cm and $z < 50$cm, where $|\rho g\left(\frac{dP_c}{dS_w}\right)^{-1}| < 0.041\ \mathrm{cm}^{-1}$ for $S_w < 0.45$.

Figures 1c, 1e, and 1f show Tests 3, 5, and 6, where the bottom of the column was open to the atmosphere while the gas was injected from the top at the prespecified pressure of 1.9, 2.2, and 2.8 kPa, respectively. Assuming a linear pressure profile for the gas phase due to the very slow gas flow, after considering the entry pressure of 1.961 kPa (20 cm water column) (see Figure 1a), the pressure gradient for gas phase is $\frac{dP_g}{dz} = 0.000$, 0.0026, and $0.0091\frac{\mathrm{kPa}}{\mathrm{cm}}$, respectively. These gas pressure gradients can be translated in terms of fluid density as $\frac{dP_g}{dz} = 0.000\,\rho g$, $0.024\,\rho g$, and $0.086\,\rho g$, respectively. The purpose of injecting gas is to drive down the capillary end effect. Figure 1c shows the water saturation profile during the secondary drainage experiment with gas injection at 1.9 kPa from the top (Test 3). In Figure 1c, the capillary end effect is reduced to the bottom 15 cm of the column due to gas injection. Smaller capillary end effect provides a larger space along the porous media for saturation data for relative permeability calculations. In addition, Figure 1c shows that a larger saturation space interval is accessible for relative permeability calculations compared to free-gravity drainage experiment (Figure 1a).

In Test 4, in addition to injecting gas at the constant pressure of 2 kPa from the top, ($\frac{dP_g}{dz} = 0.0004\frac{\mathrm{kPa}}{\mathrm{cm}} = 0.0038\,\rho g$), water was injected from the top at the constant flow rate of 2.2 cc/min for 4 h. The water flow rate was then reduced stepwise to 0.5 cc/min for an additional 4 h and finally stopped for the rest of the experiment. Figure 1d shows the saturation profile of Test 4. Compared to the previous floods, Figure 1d has a much smaller region at the bottom of the column where the water saturation is high. Or in other words, much of the capillary end effect has been removed. This allows a larger portion of the column to be used in the relative permeabilities calculations. In addition, there is no large shock moving through the system. These gradual changes in saturation allow larger water saturations to be used in the relative permeability calculations.

Figures 1e and 1f show the water saturation profiles for the secondary drainage experiments with gas injection at 2.2 and 2.8 kPa, respectively, without water influx from the top (Tests 5 and 6). These two figures show that injecting gas minimizes capillary end effect to less than 10 cm from the outlet, and larger water saturations are accessible for relative permeability calculations. The details on each experiment are listed in Table 1.

2.5.1.2. Relative Permeabilities

From each test, relative permeabilities were obtained using previously detailed method for regions where the conditions are met.

Figure 2 shows the respective two-phase water relative permeability for Tests 1–6, calculated from the saturation profiles shown in Figure 1. As mentioned above, in the case of primary free gravity drainage experiment, the water relative permeability is possible to calculate only for saturations smaller than 0.3 (see Figure 2a), while this saturation interval extends to 0.5 for secondary free gravity drainage experiment (Figure 2b). However, Figures 1c–1f show that the new method used in this work, which is providing fluid influx

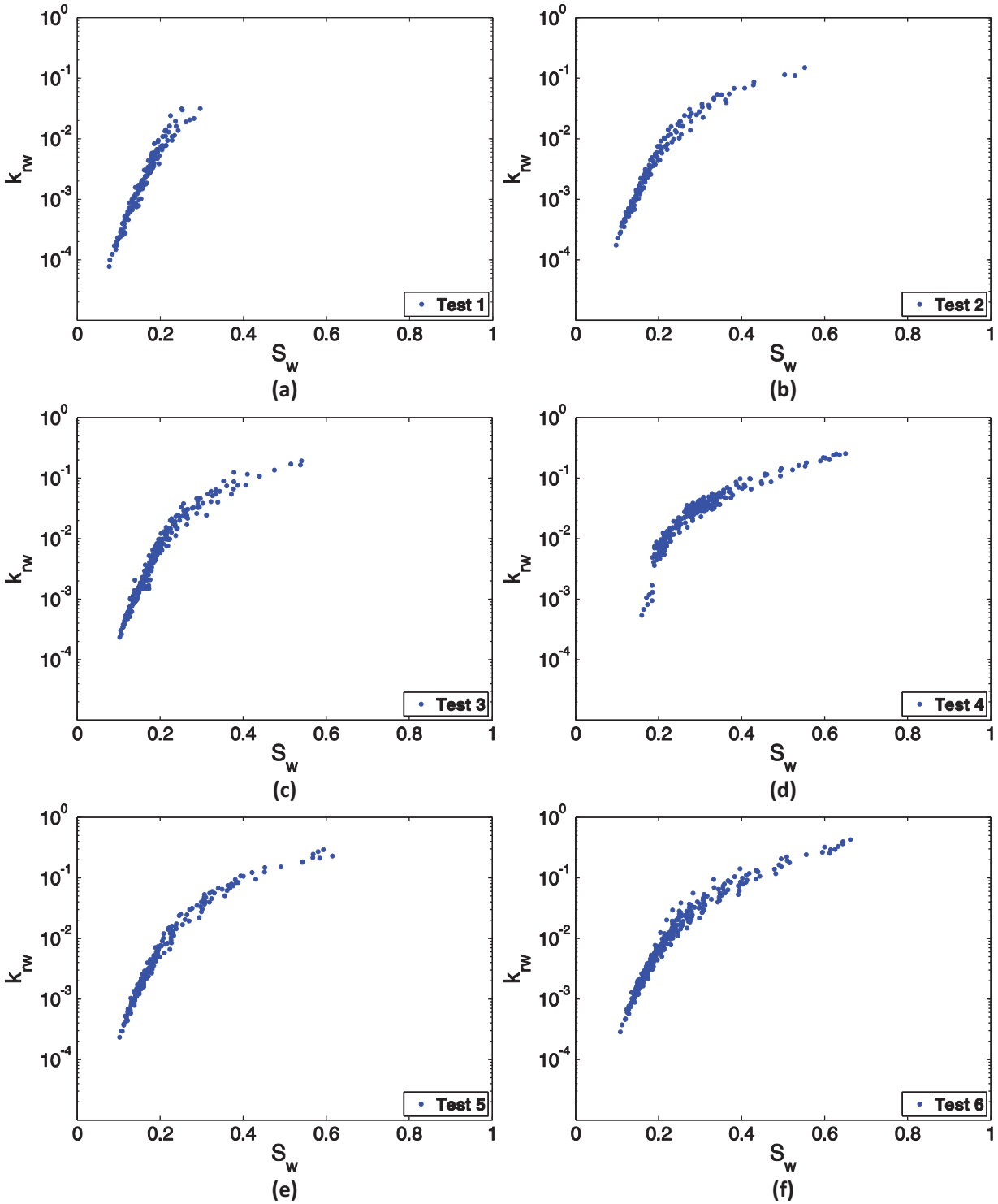

Figure 2. Two phase (water/gas) water relative permeability: (a) Test 1, (b) Test 2, (c) Test 3, (d) Test 4, (e) Test 5, and (f) Test 6.

while injecting gas, extends this saturation space to up to $S_w = 0.7$. In addition, the density of relative permeability points in midsaturation and high-saturation regions are higher which provides confidence in the reliability of the calculated relative permeability curves.

Figure 3 plots the two-phase water relative permeability measured during the two-phase gas/water experiments (Tests 1–6 shown in Table 1) in a single plot. In this figure, all the measured two-phase relative

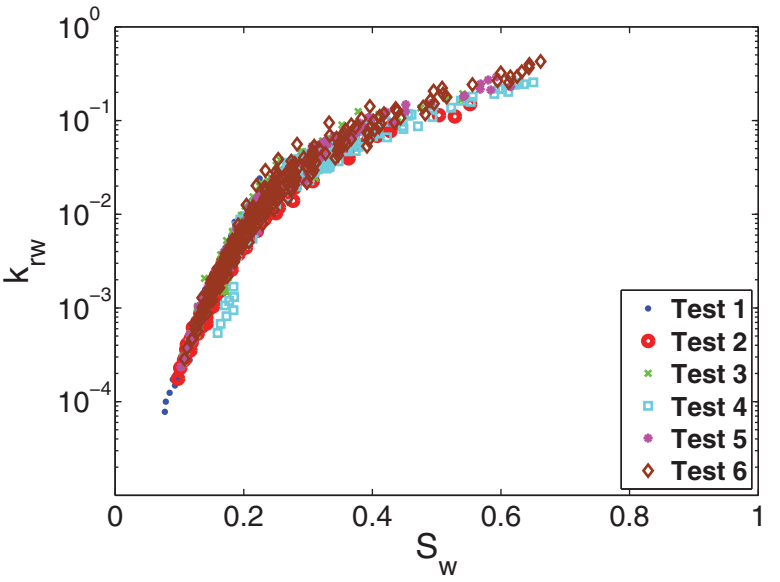

Figure 3. Two-phase water relative permeability measured during Tests 1–6.

permeability curves lie on top of each other, forming a single relative permeability curve. This single relative permeability curve confirms that the extended method used in this work, which involves injecting gas and providing fluid influxes from the top of the column is a valid procedure to measure relative permeability. Now that it is verified that our new methodology for relative permeability measurements is valid, we move forward to three-phase system to measure the effect of saturation path on relative permeability.

2.5.2. Extension of Two-Phase to Three-Phase

In the previous section, we showed that our new methodology for relative permeability measurements during two-phase experiments, involving injecting gas and providing fluid influx from the top at the same time, is a valid procedure and results in the same relative permeability curve as the previous conventional method used by *Sahni et al.* [1998] and others [*DiCarlo et al.*, 2000a, 2000b; *Dehghanpour et al.*, 2010; *Dehghanpour and DiCarlo*, 2013a]. In the next step, we extend this method further ahead to measure relative permeabilities in three-phase systems. To do this, as an analogy to two-phase measurements, we inject gas from the top at a constant pressure, while providing oil and water influxes from the top. We keep the water influx constant during each experiment, while we decrease the oil influx stepwise as we did in the two-phase experiment, Test 4. The following section presents the details of the three-phase experiments.

2.5.3. Three-Phase Experiments

The column was prepared for three-phase measurements, when it was at the final stage of the last gas/water secondary drainage experiment (Test 6). Without applying vacuum, the column was flooded with water followed by an oil flood to reach the residual water and gas saturation. This was the initial state of the column before conducting the first three-phase experiment, Test 7. For all three-phase experiments, gas was injected from the top at the constant pressure of 2 kPa while the bottom of the column was open to the atmosphere.

For Tests 8–13, the initial condition of each experiment was achieved by injecting oil and water at prespecified flow rates, and gas at 2 kPa from the top for several hours until reaching a constant oil, water, and gas saturation along the column. Next, the water injection flow rate was held constant for the entire experiment while the oil injection flow rate was reduced stepwise for a period of time to control the saturation changes. Table 2 shows the details of all three-phase experiments. Figure 4 sketches the saturation path during each three-phase experiment listed in Table 2. One can see that the three-phase experiments conducted in this work cover a large portion of the three-phase saturation space.

3. Three-Phase Results

Before presenting the three-phase relative permeability data, we show saturation profiles during one of the three-phase experiments as an example. Figure 5 shows the water and oil saturations along the

Table 2. Three-Phase Experiments With Different Initial and Conducting Conditions

Test	Type	Water Injection Rate (cc/min)	Oil Injection Rate (cc/min)	Oil Injection Period (min)
7	Secondary drainage			
8	Secondary drainage	0.375	6	105
			2	80
			0	120
9	Secondary drainage	0.6	4.875	85
			1	95
			0	250
10	Secondary drainage	0.975	5	70
			2	115
			0	210
11	Secondary drainage	1.275	2.475	90
			0	300
12	Secondary drainage	2.625	1.2	210
			0	270
13	Secondary drainage	3.75	0.675	270
			0	320

porous media during Test 9. Figure 5a indicates that water saturation is constant ($S_w \approx 0.23$) in the middle of the column ($20\,\text{cm} < z < 60\,\text{cm}$) during the entire experiment, due to the constant water influx from the top of the core (Table 2). However, the oil saturation decreases during the experiment from $S_o \approx 0.48$ to $S_o \approx 0.15$. As Figures 5a and 5b show, water and oil saturations are spatially uniform in the middle of the core ($20\,\text{cm} < z < 60\,\text{cm}$), representing a small gradient which meets the criteria mentioned above for neglecting the effect of capillary forces. In the following, we present the three-phase relative permeabilities obtained from three-phase experiments.

Figure 6 shows the calculated three-phase water relative permeability from Test 7 to 13. This is a combination of both steady state and unsteady state measurements. In particular, the unsteady state data were obtained in Test 7 (black dots), as the water saturation changes during the experiment since there is no fluid influx from the top (see Figure 4 and Table 2). As a result, we get the three-phase water relative permeability for a range of saturations using this unsteady state method. However, for the rest of three-phase experiments (Test 8–13), water is injected at a constant flow rate (see Table 2) and thus the water saturation is constant, only one data point for water relative permeability at a single water saturation is available (steady state measurement) for each experiment. Figure 6 shows that (a) there are more data points in the unsteady state portion of the data, (b) the three-phase water relative permeability calculated from both methods are identical in saturation interval 0.2–0.4, (c) the combined data form a single relative permeability curve, and (d) the relative permeability of

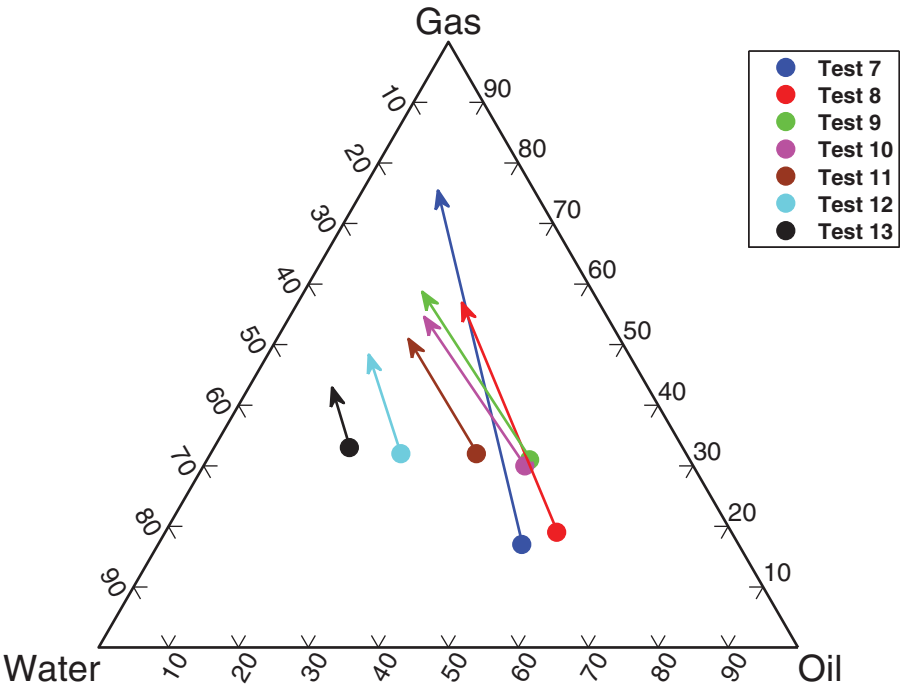

Figure 4. Saturation path covered during three-phase experiments, Tests 7–13, in the three-phase saturation space.

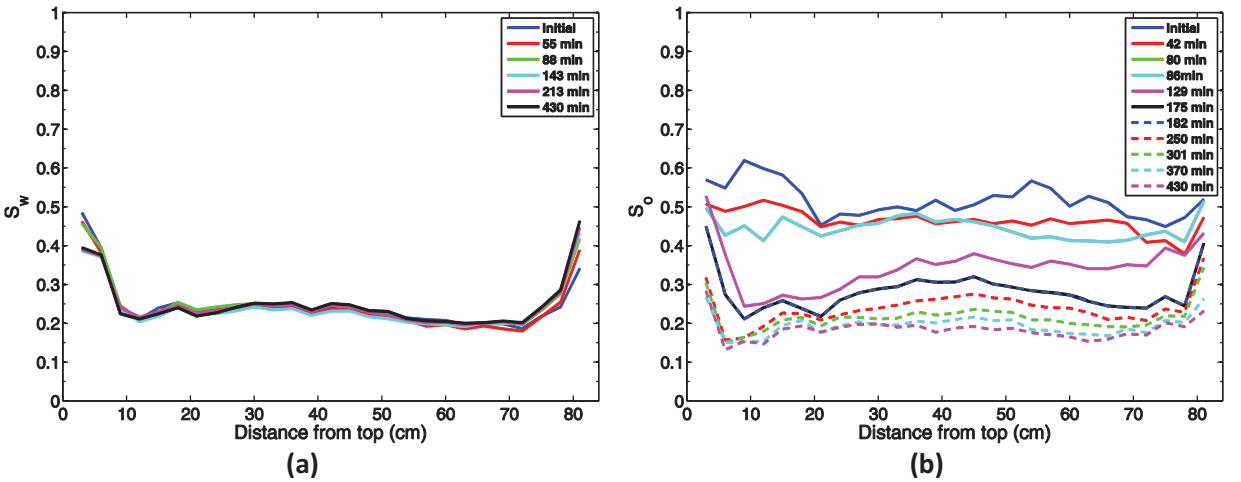

Figure 5. Water and oil saturation profiles along the sand pack column at different times during the three-phase experiment Test 9: (a) water saturation, and (b) oil saturation.

water, which is the wetting phase, is independent of saturation history and depends only on its own saturation.

In Figure 7, the two and three-phase water relative permeabilities are shown as a function of water saturation. In this figure, the three-phase water relative permeability is the same as the two-phase relative permeability in the low water saturation region ($0.1 < S_w < 0.3$). However, in the higher water saturation region, the three-phase water relative permeability is slightly lower (~7% smaller) than the two-phase water relative permeability. This observation is consistent with the observations reported by several authors [*Holmgren and Morse*, 1951; *Oak*, 1990; *Skauge and Larsen*, 1994], that the three-phase water relative permeability is slightly lower than the two-phase water relative permeability. Figure 7 however indicates that at very low water saturations ($S_w < 0.14$), the two and three-phase water relative permeability curves deviate from each other, showing a smaller three-phase water relative permeability than the two-phase. The same behavior was observed by *Sahni et al.* [1998], where three-phase water relative permeability was lower than that of the two-phase at low water saturations. One possible explanation for this behavior is that the water being the most wetting phase in a two-phase gas/water system occupies the smallest pore spaces and remains

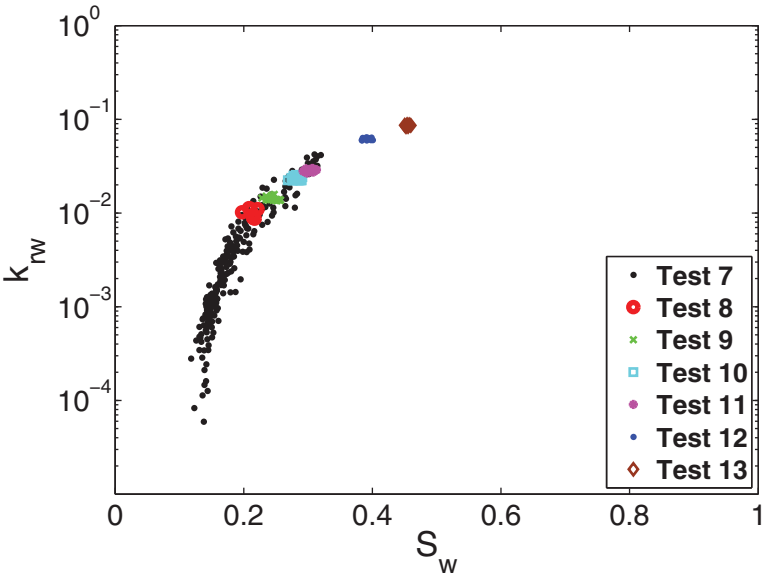

Figure 6. Steady state and unsteady state, three-phase water relative permeability measured during Tests 7–13.

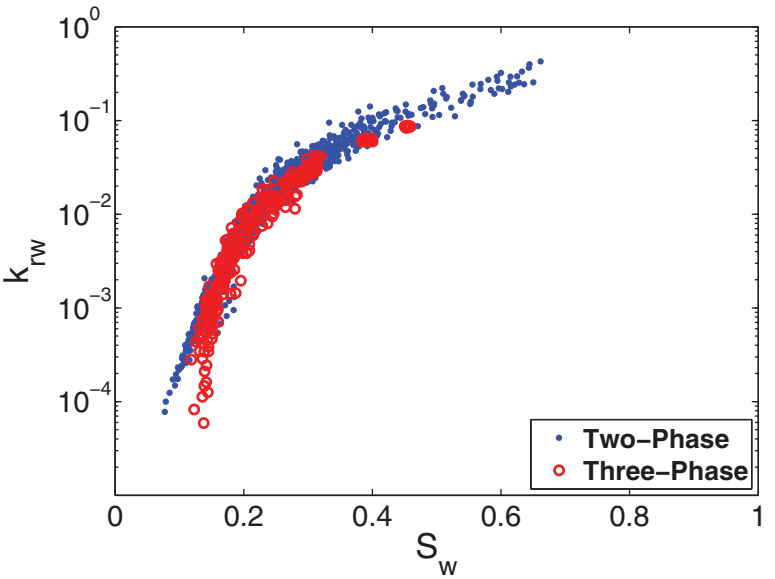

Figure 7. Two and three-phase water relative permeability.

connected even at low saturations. However, in a three-phase system, some of these smallest pores are filled with oil blobs, causing the water phase become disconnected and therefore flow difficultly. Although further investigation is necessary.

Figure 8 shows the measured three-phase oil relative permeability along different saturation paths in three-phase saturation space, Tests 7–13. The lines are fits to two different models, and are discussed later. Figure 8 shows that the oil relative permeability curves are different, depending on their saturation path in three-phase saturation space. To make these differences clearer, Figure 9 shows all the measured three-phase oil relative permeabilities shown in the Figure 8 in a single plot. In this figure, one can see that all of these relative permeability curves have similar shape, but drop to low values at different oil saturations. Moreover, Figure 9 indicates that oil relative permeability can vary orders of magnitude at the same oil saturation, depending on the saturation path. To clarify this statement, we plot only three of these relative permeability curves (for Tests 7–9) in Figure 10 to make these variations more visible. In Figure 10, the oil relative permeabilities differ orders of magnitude for different saturation paths at low saturation region ($S_o < 0.25$). For instance, in Figure 10, at $S_o = 0.2$, oil relative permeability varies from 10^{-2} to 10^{-4} moving from Test 7 to Test 9. In addition, the residual oil saturation for each of these experiments is different, depending on the saturation path. It has been known for some time that the oil relative permeability can depend on the saturation path [*Oak et al.*, 1990; *Skauge and Larsen*, 1994; *Eleri et al.*, 1995; *Fatemi et al.*, 2012]. In the following sections, we compare these results to previous measurements and give a possible explanation of the exact variations of oil relative permeability seen in these experiments.

4. Discussion

Here we fit the data to different models, going in increasing complexity, and determine the minimum amount of data that is needed to understand the three-phase relative permeabilities.

4.1. Corey-Type Fit

We first show how the Corey-type model fits our two-phase and three-phase experimental measurements. Figure 11 shows the measured two-phase water relative permeability (see Table 1) and the fit using two-phase (gas/water) Corey-type relative permeability model,

$$k_{rw} = \left(\frac{S_w - S_{wr}}{1 - S_{wr}}\right)^{n_w} \tag{9}$$

where S_{wr} is the residual water saturation and n_w is the water exponent. The Corey-type curve shown in Figure 11 uses $S_{wr} = 0.1$ and $n_w = 2.3$. The residual water saturation used for this fit is the measured residual

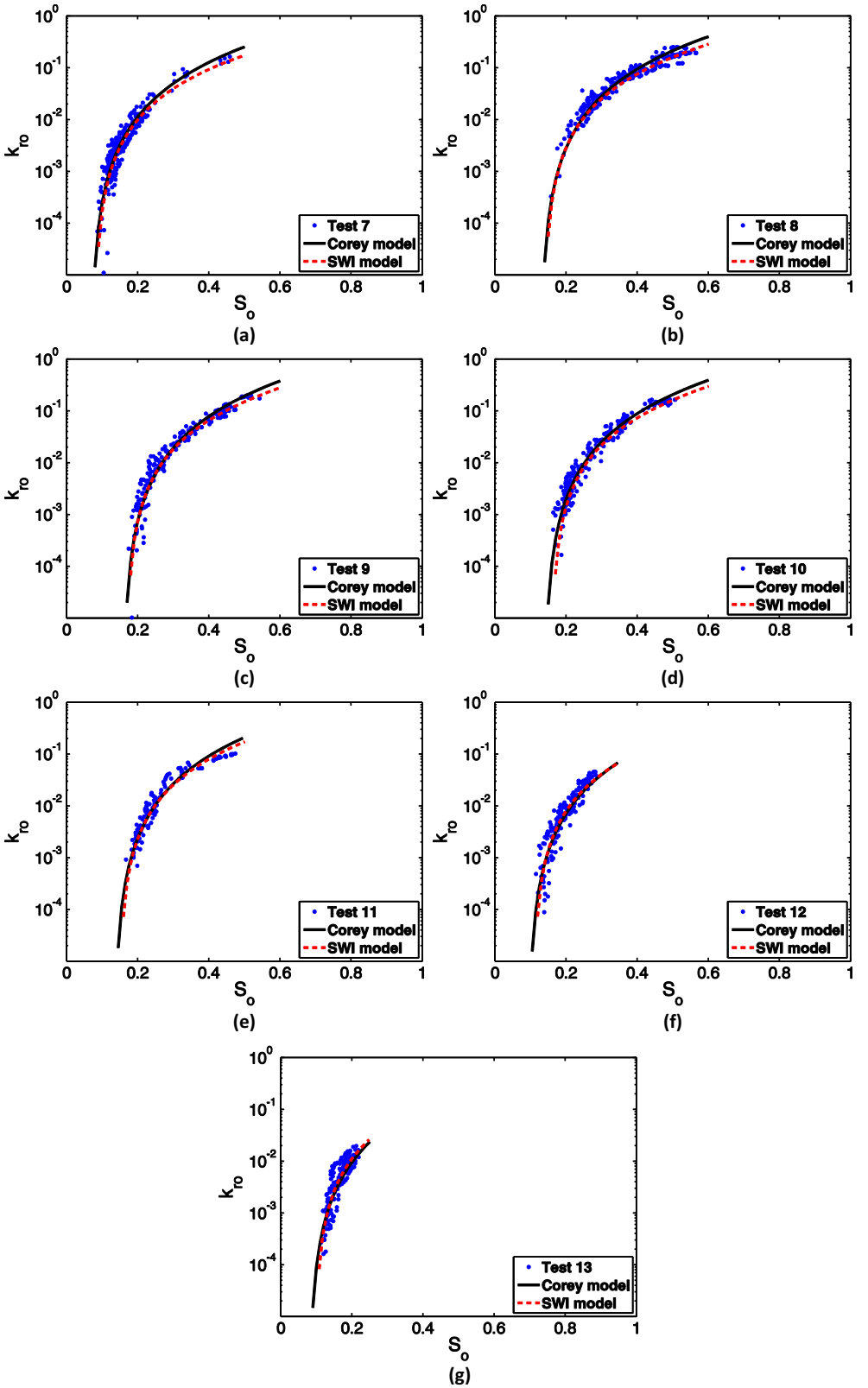

Figure 8. Three-phase oil relative permeability along different saturation paths in three-phase saturation space: (a) Test 7, (b) Test 8, (c) Test 9, (d) Test 10, (e) Test 11, (f) Test 12, and (g) Test 13. Circles show the experimental data, solid lines show Corey model fit, and dashed lines show SWI model fit.

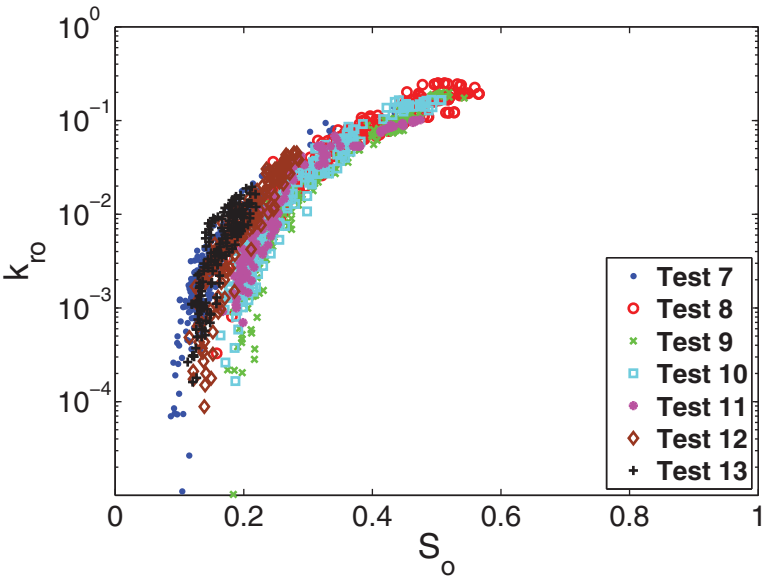

Figure 9. Three-phase oil relative permeability measured along different saturation paths in three-phase saturation space (Tests 7–13).

water saturation in the two and three-phase experiments (see Figure 1). Since water is the wetting phase, we assume that the residual water saturation is constant, and independent of number of the existing phases and saturation history [*Oak*, 1990; *Skauge and Larsen*, 1994; *Eleri et al*., 1995]. Therefore, in all of the following calculations, the residual water saturation is assumed constant and equal to 0.10.

In the next step, we match the measured three-phase oil relative permeability data during Tests 7–13, using the Corey-type model,

$$k_{ro} = C\left(\frac{S_o - S_{or}}{1 - S_{wr} - S_{or} - S_{gr}}\right)^{n_o} \tag{10}$$

where S_{or} is the residual oil saturation, S_{gr} is the residual gas saturation, n_o is the oil exponent, and C is a fitting constant. The constant $C=1$ is used for matching our experimental data, while we use other values of C for fitting other published relative permeability data presented later (section 4.4.). In addition, we measure $S_{gr}=0.1$ in

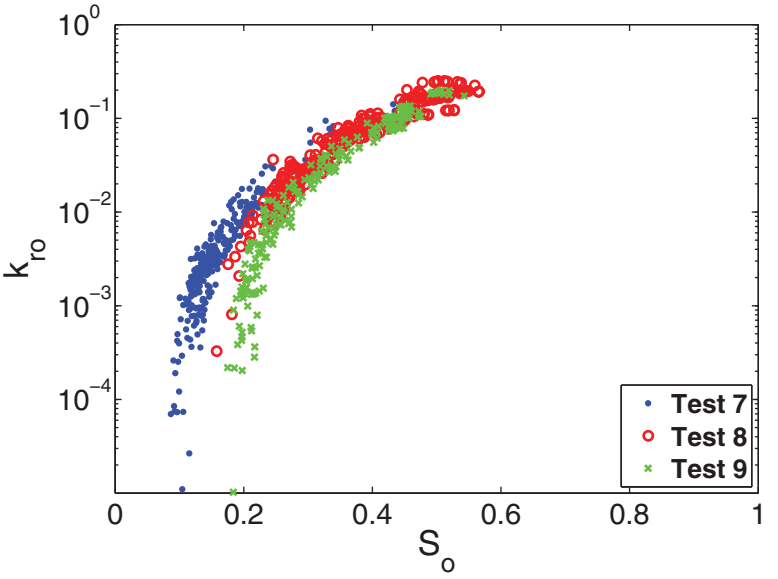

Figure 10. Three-phase oil relative permeability measured along different saturation paths in three-phase saturation space (Tests 7–9).

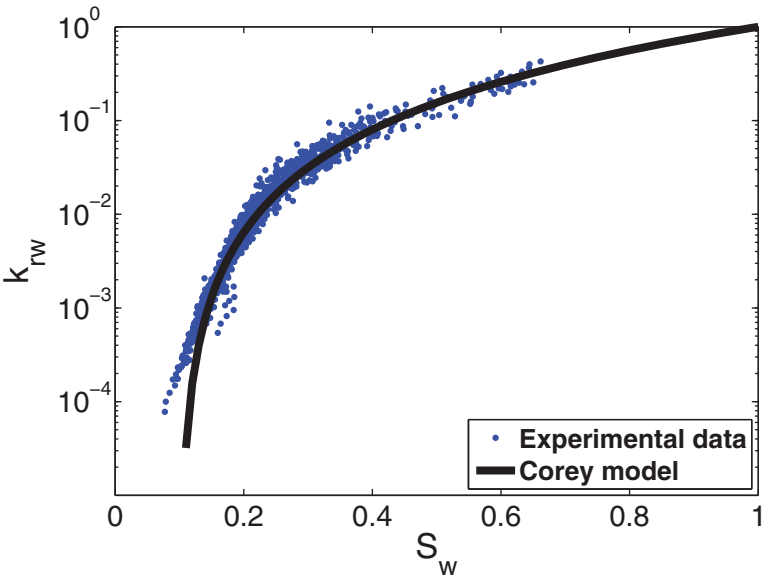

Figure 11. Two-phase water relative permeability as a function of water saturation: experimental data and Corey-type model fit.

our sand pack and use this value to match our experimental three-phase data. We first fit the Corey-type model to the measured data of Test 7 to find the oil exponent (n_o) for our porous media, and then use this exponent to match the data for Tests 8–13. Figure 8a (solid line) shows the fitted curve to the measured data for Test 7 with $n_o = 2.6$, using the residual water and gas saturations of 0.1 (explained above), the residual oil saturation of 0.07, and $C = 1$. Since the porous media is the same for all the experiments, we keep the oil exponent, residual water saturation, and residual gas saturation constant ($n_o = 2.6$, $S_{wr} = 0.1$, $S_{gr} = 0.1$, and $C = 1$) and match the experimental data for Tests 8–13 by just changing the residual oil saturation for each different saturation path experiment. Figures 8a–8g (solid line) show the fitted Corey-type model against the measured three-phase oil relative permeability data along different saturation paths (Tests 7–13). The parameters used to match the measured three-phase oil relative permeabilities by the Corey-type model are listed in Table 3. In summary, although the three-phase relative permeabilities depend on path, each three-phase relative permeability can be fit well with a simple Corey model by altering *only* the residual saturation for each path.

4.2. Saturation Weighted Interpolation Model

Since the two-phase gas/oil and oil/water relative permeabilities can differ greatly for the oil phase, it is a common practice in the petroleum industry to determine three-phase relative permeability from these measured two-phase relative permeabilities using empirical models [*Blunt*, 2000; *Blunt et al.*, 2002]. *Delshad and Pope* [1989] showed that the saturation weighted interpolation (SWI) model, first introduced by *Baker* [1988], has the best performance in predicting experimental data compared to other three-phase relative permeability models. *Baker* [1988] developed a three-phase relative permeability model based on the interpolation between the two-phase relative permeability curves,

Table 3. Corey-Type and SWI Model Parameters Used for Matching Three-Phase Oil Relative Permeability Curves

			Corey-Type Model			SWI Model			
Test	S_{wr}	S_{gr}	C	n_o	S_{or}	n_{krow}	n_{krog}	S_{or}	S_w
7	0.1	0.1	1	2.6	0.07	2	2.3	0.08	0.136
8	0.1	0.1	1	2.6	0.13	2	2.3	0.14	0.21
9	0.1	0.1	1	2.6	0.16	2	2.3	0.17	0.24
10	0.1	0.1	1	2.6	0.14	2	2.3	0.16	0.27
11	0.1	0.1	1	2.6	0.135	2	2.3	0.15	0.29
12	0.1	0.1	1	2.6	0.095	2	2.3	0.11	0.35
13	0.1	0.1	1	2.6	0.075	2	2.3	0.098	0.43

$$k_{ro}=\frac{(S_w-S_{wr})k_{ro(w)}+(S_g-S_{gr})k_{ro(g)}}{(S_w-S_{wr})+(S_g-S_{gr})} \tag{11}$$

where $k_{ro(w)}$ is the two-phase oil relative permeability to water flooding, and $k_{ro(g)}$ is the two-phase oil relative permeability to gas flooding. S_{gr} is the residual gas saturation during the two-phase oil/water experiment, which is usually zero.

Here, we use this model to fit our three-phase data. Since in the two-phase oil/gas system, oil is the wetting phase and the relative permeability of the wetting phase is independent of saturation history [*Baker*, 1988; *Delshad and Pope*, 1989; *Oak et al*., 1990; *Eleri et al*., 1995; *Blunt*, 2000], we use the measured two-phase water relative permeability curve ($k_{rw(g)}$) shown in Figure 11 as the two-phase oil relative permeability to gas flooding curve ($k_{ro(g)}$). Consequently, the two-phase oil relative permeability curve to gas flooding is

$$k_{ro(g)}=\left(\frac{S_o-S_{or}}{1-S_{or}}\right)^{n_{krog}} \tag{12}$$

where $n_{krog}=2.3$ (as explained above).

Since we did not measure the two-phase oil relative permeability to water flooding ($k_{ro(w)}$), we assume a Corey-type relative permeability curve for unconsolidated porous media,

$$k_{ro(w)}=\left(\frac{S_o-S_{or}}{1-S_{wr}-S_{or}}\right)^{n_{krow}} \tag{13}$$

where $n_{krow}=2$[*Honarpour et al*., 1986; *Honarpour and Mahmood*, 1988; *Dehghanpour and DiCarlo*, 2013a].

With these curves, we use the same approach as the Corey-type model to fit the measured three-phase oil relative permeability curves using SWI. We match the measured three-phase oil relative permeability curves by only changing the residual oil saturation (S_{or}). We change the residual oil saturation (S_{or}) in both $k_{ro(g)}$ and $k_{ro(w)}$ equations (equations (12) and (13)) for each three-phase experiment, and then use them in SWI model (equation (11)). Since the water saturation during each three-phase experiment is almost constant (Figure 4), the final water saturation of each experiment is the water saturation (S_w) used in SWI model (equation (11)). Figure 8 shows the measured relative permeability data and the SWI model match (dashed line). It is clear that, in this case, the same as the Corey-type model, changing residual saturations results in a match with measured data. The parameters used in matching the measured data with SWI model are given in Table 3.

Additionally, this shows that for SWI to fit the data, the residual oil saturation *must* be altered. Just using the two-phase relative permeabilities is not enough as the measured relative permeability changes more than the two-phase relative permeability at low oil saturation.

4.3. Results in Context of Oil Relative Permeability Functionality

The assumptions behind the commonly used three-phase relative permeability models, i.e., Stone I and II, Parker, Corey, and Baker are that in a water-wet media, the relative permeability of water and gas are a function of their own saturation, whereas the relative permeability of oil is a function of two saturations [*Fayers and Matthews*, 1984; *Delshad and Pope*, 1989; *Oak*, 1990]. Stone I and II [*Stone*, 1970, 1973] assume a linear relationship between mobile oil saturation and gas saturation [*Fayers and Matthews*, 1984]. The Parker model [*Parker et al*., 1987] assumes the same functionality for three-phase oil relative permeability, while assuming the residual fluid saturations are independent of saturation history. The Baker model [*Baker*, 1988] uses a saturation weighted interpolation (SWI) method to predict three-phase relative permeability from two-phase data. The Corey model [*Brooks and Corey*, 1964] however treats the dependence of oil relative permeability on two saturations differently. This model applies this assumption through the dependence of the residual oil saturation on two saturations, i.e., $S_{or}=f(S_w,S_g)$ [*Brooks and Corey*, 1964; *Delshad and Pope*, 1989].

Several authors examined the assumption of dependence of oil relative permeability on two saturations against experimental data. *Fayers and Matthews* [1984] explored this assumption by examining the performance of Stone I and II models against seven experimental data sets. They found that both Stone models fail at low saturations where oil saturation approaches residual saturation. *Delshad and Pope* [1989] conducted

a detailed study on the performance of all of the above mentioned models against five experimental data sets. They found that these models often do not accurately predict the experimental data. Other authors [*Baker*, 1988; *Oak*, 1990; *Oak et al*., 1990] also reported the same inaccuracies regarding the Stone model for predicting experimental data. The comprehensive studies by *Baker* [1988] and *Delshad and Pope* [1989] make it clear that saturation weighted interpolation (SWI) method is the best model available [*Blunt*, 2000]. This is why we used SWI model in this study.

But most importantly, *Delshad and Pope* [1989] found that their data set did not completely support the assumption of dependency of oil relative permeability on two saturations. In addition, *Fayers and Matthews* [1984] concluded that the residual saturations are not a linear function of gas and water saturation, and experimental measurements of residual oil saturation at variety of water and gas saturations are required.

The results of our study are in agreement with the conclusions by *Delshad and Pope* [1989] and *Fayers and Matthews* [1984]. As mentioned earlier, the three-phase oil relative permeability data shown in Figure 9 indicate that the oil relative permeability curves have similar shape while the residual oil saturations are different. In fact, Figure 9 suggests that oil relative permeability is mainly a function of its own saturation. However, there must be another parameter in oil relative permeability functionality which causes different relative permeabilities, for different saturation paths (see Figures 9 and 10). On the other hand, in previous sections, we showed that by using different residual oil saturation for each saturation path, Corey and SWI models are capable of fitting our experimental data (see Figure 8). Consequently, our results suggest that oil relative permeability is only a function of oil saturation, while the residual oil saturation is a function of saturation path and depends on the saturation of other phases. The functionality of residual oil saturation is discussed later in section 4.5.

4.4. Comparison to Other Published Three-Phase Oil Relative Permeability

Due to laboratory difficulties of three-phase relative permeability measurements, published data on three-phase relative permeabilities are not plentiful. Moreover, the reported relative permeability data are mostly incomplete sets of data and do not include the saturation paths in three-phase saturation space. Among the published three-phase relative permeability data, we use two data sets reported by *Oak et al*. [1990] and *Eleri et al*. [1995] to examine the findings from our own experimental data presented in this paper. We select these two data sets since they provide saturation paths for their experiments, and use water-wet rocks.

Oak et al. [1990] conducted various two and three-phase relative permeability measurements using steady state method on water-wet, Berea sandstone with permeability of 210–160 md. On the other hand, *Eleri et al*. [1995] used unsteady state method to measure three-phase relative permeability in a water-wet, Clashach core with 234 md. Figure 12 shows the initial and final saturation of each experiment in three-phase space reported by *Oak et al*. [1990] and *Eleri et al*. [1995].

We use the Corey model to fit the reported three-phase oil relative permeabilities. With the same approach used in section 4.1, we first fit the first relative permeability curve using equation (10). We then keep S_{wr}, S_{gr} and $n_o$constant, and try to fit the other curves by just changing the residual oil saturation (S_{or}).

Figure 13 shows the three-phase relative permeability data reported by *Oak et al*. [1990] and their respective Corey model fits. *Oak et al*. [1990] reported a residual water saturation of their rock as $S_{wr}=0.3$. In addition, Figure 12 shows that both of their experiments started at $S_g=0$. Therefore, we use $S_{gr}=0$ in equation (10) to model their data by the Corey model, as for these saturation paths, maximum possible oil saturation is $S_{o,\max}=1-S_{wr}$. Using the same residual water and residual gas saturations, we fit the first relative permeability data by using $n_o=4$, $S_{or}=0.08$, and $C=2.5$ (solid line, Figure 13). To fit the second curve, we only change the residual oil saturation to $S_{or}=0.18$. The dashed line in Figure 13 shows that the model fits the experimental data of the second experiment well. The used parameters to fit the experimental data are listed Table 4.

We use the same approach to fit the experimental data reported by *Eleri et al*. [1995] using the Corey model (equation (10)). They reported $S_{wr}=0.21$ for their core. Figure 12 shows that their first experiment started at $S_g=0$, while the other two start at $S_g=0.10$ and $S_g=0.12$, respectively. Therefore, we use $S_{gr}=0$ for their first experiment, and $S_{gr}=0.1$ for the other two in equation (10) to model their oil relative permeability data by the Corey model. Thus, we used $S_{wr}=0.21$, and $S_{gr}=0$ along with $S_{or}=0.215$, $n_o=2.5$, and $C=0.7$ to fit the

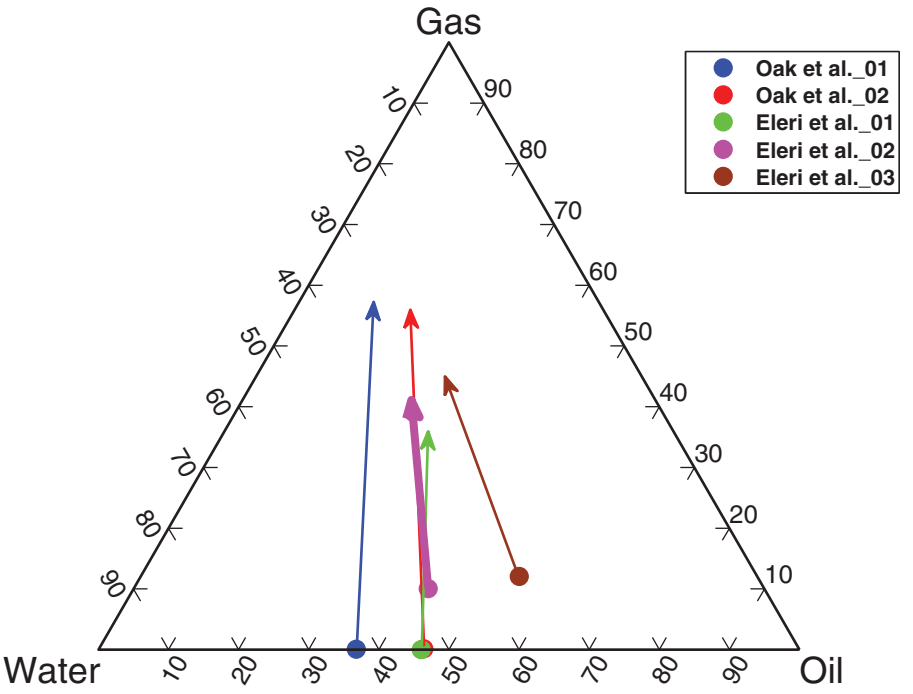

Figure 12. Initial and final saturation of three-phase experiments reported by *Oak et al.* [1990], and *Eleri et al.* [1995] in the three-phase saturation space.

first relative permeability curve reported by them. The experimental data along with their respective Corey model fit are shown in Figure 14. By simply changing the residual oil saturations to $S_{or}=0.16$ and $S_{or}=0.18$, the model fits the experimental data (see Figure 14). The used parameters to fit the experimental data are listed Table 4.

The presented experimental data with the Corey model fits match our findings from our own experimental measurements presented in this work. The oil relative permeability data measured by others *Oak et al.*

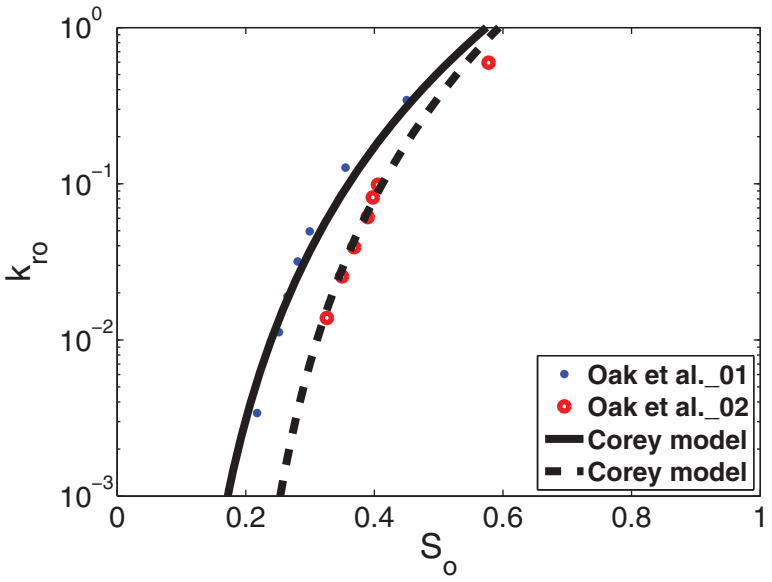

Figure 13. Points and circles: three-phase oil relative permeability reported by *Oak et al.* [1990]; solid and dashed lines: Corey-model fits to *Oak et al.* [1990] experimental data.

Table 4. Corey-Type Model Parameters Used for Matching Three-Phase Oil Relative Permeability Curves Reported by *Oak et al.* [1990] and *Eleri et al.* [1995]

Test	C	S_{wr}	S_{gr}	n_o	S_{or}
Oak et al. _ 01	2.5	0.3	0	4	0.08
Oak et al. _ 02	2.5	0.3	0	4	0.18
Eleri et al. _ 01	0.7	0.21	0	2.5	0.215
Eleri et al. _ 02	0.7	0.21	0.1	2.5	0.16
Eleri et al. _ 03	0.7	0.21	0.1	2.5	0.18

[1990] and *Eleri et al.* [1995] suggest that, by only changing the residual oil saturation, standard relative permeability models (Corey model here) can fit the experimental data.

4.5. Three-Phase Relative Permeability and Connectivity of Phases at Small Scales

Our three-phase oil relative permeability presented in previous section show that the oil relative permeability differs orders of magnitude at the same oil saturation depending on the saturation path in three-phase saturation space, while the residual oil saturation for each saturation path is different.

Figure 15 shows the residual oil saturation as a function of final water saturation in the system used to fit the experimental data by the Corey-type and SWI models. Figure 15 shows an increasing and decreasing trend in residual oil saturation as the final water saturation increases. Figure 16 shows the final oil saturation as a function of final water saturation for a series of water and gas floods in a Clashach, water wet rock reported by *Eleri et al.* [1995]. The data in Figure 16 show the same increasing and decreasing residual oil saturation as a function of final water saturation, as observed in our experiments (see Figure 15).

In a water-wet media, the water phase occupies the smallest pores regardless of the other phases. This behavior results in the independency of the water relative permeability from other phases saturations and saturation path, as was seen in this work (see Figure 7) and confirmed by others [*Oak*, 1990; *Fayers and Matthews*, 1984; *Eleri et al.*, 1995]. On the other hand, the oil phase being the intermediate-wetting phase occupies the midsize pores. Consequently, the oil relative permeability depends on the saturation of more than one phase, and the saturation path, as was observed in this work (see Figure 9) and others [*Oak*, 1991; *Fayers and Matthews*, 1984; *DiCarlo et al.*, 2000a, 2000b].

This type of fluids distribution in pore spaces can explain the increasing-decreasing behavior of residual oil saturation seen in Figures 15 and 16. At low water saturations, the water phase occupies the smallest pore sizes, leaving medium and large-size pores available for oil and gas phases. In this case, oil phase occupies intermediate-size pores forming layers between water and gas phase. In this low water saturation region, the layer drainage regime previously observed experimentally and confirmed theoretically by others [*Grader and O'Meara*, 1988; *Naylor et al.*, 1996; *Keller et al.*, 1997; *Zhou and Blunt*, 1997; *Sahni et al.*, 1998; *DiCarlo et al.*, 2000a, 2000b; *Piri and*

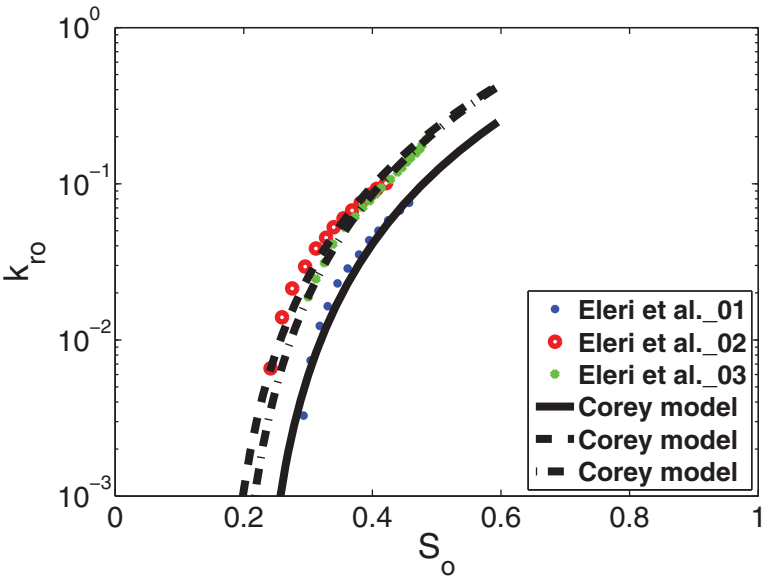

Figure 14. Points, circles, and crosses: three-phase oil relative permeability reported by *Eleri et al.* [1995]; solid, dashed, and dotted lines: Corey-model fits to *Eleri et al.* [1995] experimental data.

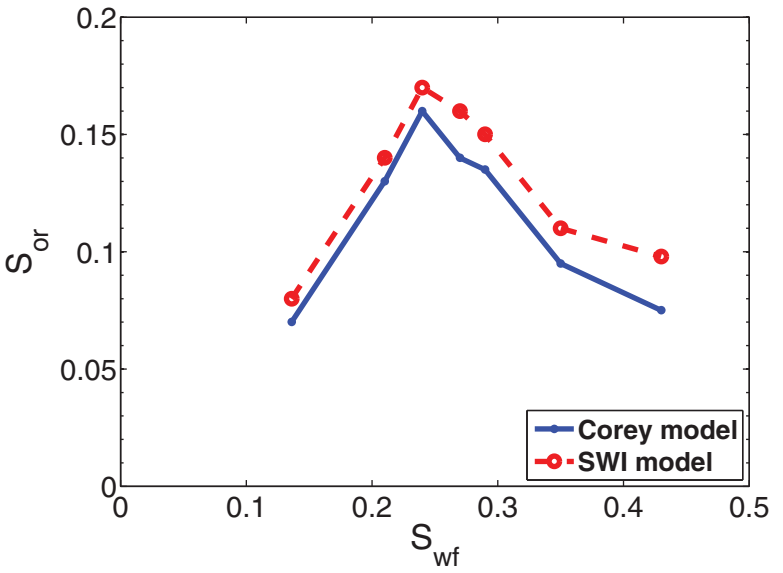

Figure 15. Residual oil saturation as a function of final water saturation measured in this work.

Blunt, 2005a; *Piri and Blunt*, 2005b; *Ghanbarian-Alavijeh and Hunt*, 2012; *Ghanbarzadeh et al.*, 2014] govern the flow which results in lower residual oil saturations. As the water saturation increases, the water and oil phases compete for occupying intermediate-size pores resulting in the trapping of oil phase among water phase. This explains the higher residual oil saturation in the middle water saturation region in Figures 15 and 16. Finally, as the saturation of water phase increases, all the intermediate-size pores will be occupied by water, leaving oil phase no choice other than occupying large size pores. This will consequently result in decreasing residual oil saturations as it is easier for the oil phase to move in larger pores. This can be explained by the results of *Alizadeh and Piri* [2014], where they did not observe any changes in three-phase oil relative permeability for different saturation histories in their water-wet medium. They attributed the independency of their three-phase oil relative permeability to saturation history, to the narrow pore-size distribution of their sandstone rock.

Overall, this work suggests that in the gravity drainage regime in our sand pack and the two water-wet sandstone rocks studied by *Oak et al*. [1990] and *Eleri et al*. [1995], the connectivity of the flowing fraction of each phase is the only important part which determines the relative permeability of each phase. To put this

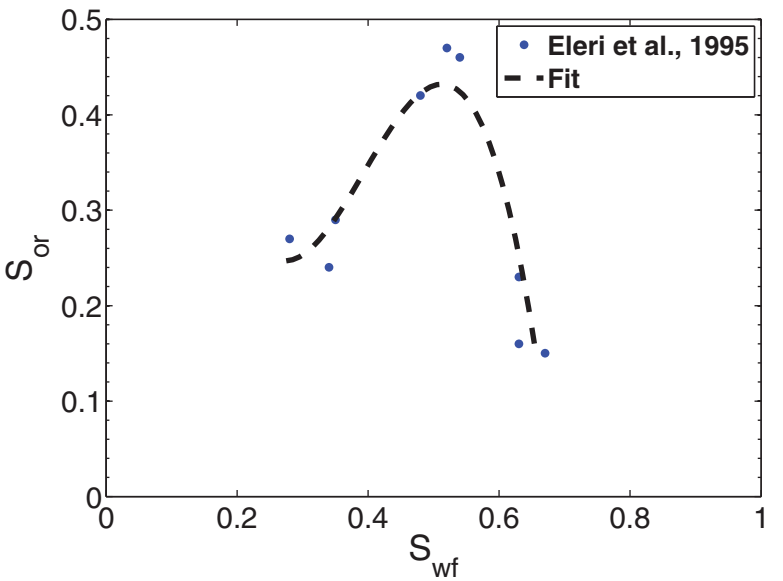

Figure 16. Residual oil saturation as a function of final water saturation measured by *Eleri et al.* [1995].

statement in a more technical terminology, our results and measurements reported by others [*Oak et al*., 1990; *Eleri et al*. 1995] support that the key parameter in three-phase oil relative permeability is the residual oil saturation in presence of other phases. In fact, the results of this work show that the three-phase oil relative permeability is only a function of oil saturation if the residual oil saturation changes are accounted for accordingly, depending on the saturation path in the three-phase space.

5. Summary and Conclusions

In this work, we measured three-phase oil relative permeabilities along various saturation paths in three-phase saturation space in order to quantify the effect of saturation path on the oil phase relative permeability. We observed that, depending on the saturation path of each experimental measurement, the three-phase oil relative permeability can change orders of magnitude, at the same oil saturation, in the same porous media. It was surprising to the authors that it is possible to have relative permeabilities several orders of magnitude different at the same saturations. We later examined the performance of three-phase relative permeability models in prediction of our experimental three-phase relative permeability data to see if this observation can be described by these standard models. We tested two three-phase relative permeability models, namely Corey-type and SWI, against our experimental measurements. These models matched our experimental data well, once we changed the residual oil saturations appropriately for each saturation paths. We compared our results to previously published three-phase oil relative permeabilities by using the same approach to fit the reported experimental data. The standard Corey-type model was able to fit the data by only fixing residual oil saturations. Our measurements suggest that, three-phase oil relative permeability is only a function of oil saturation while the residual oil saturation is a function of saturation of other phases, i.e., water saturation. Our results indicate that, with correct estimate of residual saturations for each saturation path in three-phase phase space, these two standard relative permeability models are capable of predicting the relative permeabilities correctly.

Notation

C	fitting constant (dimensionless)
g	gravity (m/s^2)
k	absolute permeability (darcy)
k_{ri}	relative permeability to phase i (dimensionless)
$k_{ro(g)}$	oil relative permeability to gas flooding (dimensionless)
$k_{ro(w)}$	oil relative permeability to water flooding (dimensionless)
n_i	phase i exponent for relative permeability (dimensionless)
P_c	capillary pressure (Pa)
P_i	pressure of phase i (Pa)
S_i	saturation of phase i (dimensionless)
S_{gr}	residual gas saturation (dimensionless)
S_{or}	residual oil saturation (dimensionless)
S_{wr}	residual water saturation (dimensionless)
u_i	flux of phase i (m/s)
z	position along porous media

Greek Letters

μ_i	viscosity of phase i (cp)
ρ_i	density of phase i (kg/m3)
Φ_i	potential of phase i (Pa)
ϕ	porosity (dimensionless)

Subscripts

i	phase
j	time step
g	gas
o	oil
w	water

Acknowledgments
We gratefully acknowledge the gas—enhanced oil recovery joint industry project (JIP) at the University of Texas at Austin for their financial support of this work. The relative permeability versus saturation data are available upon request by emailing David A. DiCarlo or Amir Kianinejad at dicarlo@mail.utexas.edu or kianinejad.amir@utexas.edu.

References

Akbarabadi, M., and M. Piri (2013), Relative permeability hysteresis and capillary trapping characteristics of supercritical CO_2/brine systems: An experimental study at reservoir conditions, *Adv. Water Resour.*, *52*, 190–206, doi:10.1016/j.advwatres.2012.06.014.

Akin, S., and M. R. B. Demiral (1997), Effect of flow rate on imbibition three-phase relative permeabilities and capillary pressures, paper SPE-38897-MS presented at SPE Annual Technical Conference and Exhibition, Society of Petroleum Engineers, San Antonio, Tex., 5–8 Oct., doi:10.2118/38897-MS.

Alizadeh, A. H., and M. Piri (2014), The effect of saturation history on three-phase relative permeability: An experimental study, *Water Resour. Res.*, *50*, 1636–1664, doi:10.1002/2013WR014914.

Aminzadeh-goharrizi, B., D. A. DiCarlo, D. H. Chung, A. Kianinejad, S. L. Bryant, C. Huh, and M. Roberts (2012), Effect of nanoparticles on flow alteration during CO_2 injection, paper SPE-160052-MS presented at SPE Annual Technical Conference and Exhibition, Society of Petroleum Engineers, San Antonio, Tex., 5–8 Oct., doi:10.2118/160052-MS.

Baker, L. E. (1988), Three-phase relative permeability correlations, paper SPE-17369-MS presented at SPE Enhanced Oil Recovery Symposium, Society of Petroleum Engineers, Tulsa, Okla., 16–21 Apr.

Beygi, M. R., M. Delshad, V. S. Pudugramam, G. A. Pope, and M. F. Wheeler (2015), Novel three-phase compositional relative permeability and three-phase hysteresis models, *SPE J., SPE-165324-PA*, doi:10.2118/165324-PA.

Blunt, M. J. (2000), An empirical model for three-phase relative permeability, *SPE J.*, *5*(4), 435–445.

Blunt, M. J., M. D. Jackson, M. Piri, and P. H. Valvatne (2002), Detailed physics, predictive capabilities and macroscopic consequences for pore-network models of multiphase flow, *Adv. Water Resour.*, *25*(8), 1069–1089.

Brooks, R. H., and A. T. Corey (1964), *Hydraulic Properties of Porous Media*, Colo. State Univ., Fort Collins, Colo.

Carlson, F. M. (1981), Simulation of relative permeability hysteresis to the nonwetting phase, paper SPE-10157-MS presented at SPE Annual Technical Conference and Exhibition, Society of Petroleum Engineers, San Antonio, Tex., 4–7 Oct.

Chen, X., A. Kianinejad, and D. A. DiCarlo (2014), An experimental study of CO_2-brine relative permeability in sandstone, paper SPE-169137-MS presented at in SPE Improved Oil Recovery Symposium, Society of Petroleum Engineers, Tulsa, Okla., doi:10.2118/169137-MS.

Dehghanpour, H. (2011), Measurement and modeling of three-phase oil relative permeability, Ph.D. dissertation, The Univ. of Tex. at Austin, Austin, Tex.

Dehghanpour, H., and D. A. DiCarlo (2013a), A comparative study of transient and steady-state three-phase oil permeability, *J. Can. Pet. Technol.*, *52*(1), 54–63.

Dehghanpour, H., and D.A. DiCarlo (2013b), Drainage of capillary-trapped oil by an immiscible gas: Impact of transient and steady-state water displacement on three-phase oil permeability, *Transp. Porous Media*, *100*(2), 297–319, doi:10.1007/s11242-013-0217-z.

Dehghanpour, H., D. A. DiCarlo, B. Aminzadeh, and M. Mirzaei Galeh-Kalaei (2010), Two-phase and three-phase saturation routes and relative permeability during fast drainage, paper SPE-129962-MS presented at SPE Improved Oil Recovery Symposium, Society of Petroleum Engineers, Tulsa, Okla., 24–28 Apr.

Dehghanpour, H., B. Aminzadeh, M. Mirzaei, and D. A. DiCarlo (2011), Flow coupling during three-phase gravity drainage, *Phys. Rev. E*, *83*(6), 065302.

Delshad, M., and G. A. Pope (1989), Comparison of the three-phase oil relative permeability models, *Transp. Porous Media*, *4*(1), 59–83.

DiCarlo, D. A., A. Sahni, and M. J. Blunt (2000a), Three-phase relative permeability of water-wet oil-wet and mixed-wet sandpacks, *SPE J.*, *5*(1), 82–91.

Dicarlo, D. A., A. Sahni, and M. J. Blunt (2000b), The effect of wettability on three-phase relative permeability, *Transp. Porous Media*, *39*(3), 347–366.

Eleri, O. O., A. Graue, and A. Skauge (1995a), Steady-state and unsteady-state two-phase relative permeability hysteresis and measurements of three-phase relative permeabilities using imaging techniques, paper SPE-30764-MS presented at SPE Annual Technical Conference and Exhibition, Society of Petroleum Engineers, Dallas, Tex., 22–25 Oct.

Eleri, O. O., A. Graue, A. Skauge, and J. A. Larsen (1995b), Calculation of three-phase relative permeabilities from displacement experiments with measurements of in-situ saturation, paper SCA 9509 presented at the International Symposium of the Society of Core Analysts, San Francisco, California, 12–14 Sept.

Fassihi, M. R., and G. F. Potter (2009), Analysis of transient data during relative permeability measurements using steady-state technique, paper SPE-123676-MS presented at SPE Annual Technical Conference and Exhibition, Society of Petroleum Engineers, New Orleans, La., 4–7 Oct.

Fatemi, S. M., M. Sohrabi, M. Jamiolahmady, S. Ireland, and G. Robertson (2011), Experimental investigation of near-miscible water-alternating-gas (WAG) injection performance in water-wet and mixed-wet systems, paper SPE-145191-MS presented at Offshore Europe, Society of Petroleum Engineers, Aberdeen, U. K., 6–8 Sept.

Fatemi, S. M., M. Jamiolahmady, M. Sohrabi, and S. Ireland (2012), Cyclic hysteresis of three-phase relative permeability applicable to WAG injection: Water-wet and mixed-wet systems under low gas/oil IFT, paper SPE-159816-MS presented at SPE Annual Technical Conference and Exhibition, Society of Petroleum Engineers, San Antonio, Tex., 8–10 Oct.

Fayers, F. J., and J. D. Matthews (1984), Evaluation of normalized Stone's methods for estimating three-phase relative permeabilities, *SPE J.*, *24*(2), 224–232.

Ghanbarian-Alavijeh, B., and A. G. Hunt (2012), Comparison of the predictions of universal scaling of the saturation dependence of the air permeability with experiment, *Water Resour. Res.*, *48*, W08513, doi:10.1029/2011WR011758.

Ghanbarzadeh, S., M. Prodanović, and M. A. Hesse (2014), Percolation and grain boundary wetting in anisotropic texturally equilibrated pore networks, *Phys. Rev. Lett.*, *113*(4), 048001.

Grader, A. S., and D. J. O'Meara Jr. (1988), Dynamic displacement measurements of three-phase relative permeabilities using three immiscible liquids, paper SPE-18293-MS presented at SPE Annual Technical Conference and Exhibition, Society of Petroleum Engineers, Houston, Tex., 2–5 Oct.

Holmgren, C. R., and R. A. Morse (1951), Effect of free gas saturation on oil recovery by water flooding, *J. Pet. Technol.*, *3*(5), 135–140.

Honarpour, M., and S. M. Mahmood (1988), Relative-permeability measurements: An overview, *J. Pet. Technol.*, *40*(8), 963–966.

Honarpour, M., L. F. Koederitz, and A. H. Harvey (1986), *Relative Permeability of Petroleum Reservoirs*, CRC Press, Boca Raton, Fla.

Hosseini, S. A., H. Lashgari, J. W. Choi, J. Nicot, J. Lu, and S. D. Hovorka (2013), Static and dynamic reservoir modeling for geological CO_2 sequestration at Cranfield, Mississippi, USA, *Int. J. Greenhouse Gas Control*, *18*, 449–462.

Huyakorn, P. S., S. Panday, and Y. S. Wu (1994), A three-dimensional multiphase flow model for assessing NAPL contamination in porous and fractured media, 1. Formulation, *J. Contam. Hydrol.*, *16*(2), 109–130.

Jerauld, G. R. (1997), General three-phase relative permeability model for Prudhoe Bay, *SPE Reservoir Eng.*, *12*(4), 255–263.

Johnson, E. F., D. P. Bossler, and V.O. Naumann (1959), Calculation of relative permeability from displacement experiments, *Am. Inst. Min. Metall. Pet. Eng., SPE-1023-G*, *216*, 370–372.
Jones, S. C., and W. O. Roszelle (1978), Graphical techniques for determining relative permeability from displacement experiments, *J. Pet. Technol.*, *30*(5), 807–817, doi:10.2118/6045-PA.
Juanes, R., E. J. Spiteri, F. M. Orr, and M. J. Blunt (2006), Impact of relative permeability hysteresis on geological CO_2 storage, *Water Resour. Res.*, *42*, W12418, doi:10.1029/2005WR004806.
Keller, A. A., M. J. Blunt, and P. V. Roberts (1997), Micromodel observation of the role of oil layers in three-phase flow, *Transp. Porous Media*, *26*(3), 277–297.
Kianinejad, A., B. Aminzadeh, X. Chen, and D. A. DiCarlo (2014), Three-phase relative permeabilities as a function of flow history, paper SPE-169083-MS presented at SPE Improved Oil Recovery Symposium, Society of Petroleum Engineers, Tulsa, Okla., 12–16 Apr., doi:10.2118/169083-MS.
Krevor, S. C. M., R. Pini, L. Zuo, and S. M. Benson (2012), Relative permeability and trapping of CO_2 and water in sandstone rocks at reservoir conditions, *Water Resour. Res.*, *48*, W02532, doi:10.1029/2011WR010859.
Kuo, C., and S. M. Benson (2015), Numerical and analytical study of effects of small scale heterogeneity on CO_2/brine multiphase flow system in horizontal corefloods, *Adv. Water Resour.*, *79*, 1–17, doi:10.1016/j.advwatres.2015.01.012.
Land, C. S. (1968), Calculation of imbibition relative permeability for two- and three-phase flow from rock properties, *SPE J.*, *8*(2), 149–156, doi:10.2118/1942-PA.
Larsen, J. A., and A. Skauge (1995), Comparing hysteresis models for relative permeability in WAG studies, *paper SCA 9506 presented at the International Symposium of the Society of Core Analysts,* San Francisco, Calif., 12–14 Sept.
Larsen, J. A., and A. Skauge (1998), Methodology for numerical simulation with cycle-dependent relative permeabilities, *SPE J.*, *3*(2), 163–173, doi:10.2118/38456-PA.
Mohanty, K. K., and A. E. Miller (1991), Factors influencing unsteady relative permeability of a mixed-wet reservoir rock, *SPE Form. Eval.*, *6*(3), 349–358.
Mohsenzadeh, A., M. Nabipour, S. Asadizadeh, M. Nekouie, A. Ameri, and S. Ayatollahi (2011), Experimental investigation of different steam injection scenarios during SAGD process, *Spec. Top. Rev. Porous Media Int. J.*, *2*(4), 283–291, doi:10.1615/SpecialTopicsRevPorousMedia.v2.i4.30.
Mohsenzadeh, A., M. Escrochi, M. V. Afraz, A. Y. Mansoor, and S. Ayatollahi (2012), Experimental investigation of heavy oil recovery from fractured reservoirs by secondary steam-gas assisted gravity drainage, paper SPE-157202-MS presented at SPE Heavy Oil Conference Canada, Society of Petroleum Engineers, Calgary, Alberta, Canada, 12–14 June, doi:10.2118/157202-MS.
Moortgat, J., S. Sun, and A. Firoozabadi (2011), Compositional modeling of three-phase flow with gravity using higher-order finite element methods, *Water Resour. Res.*, *47*, W05511, doi:10.1029/2010WR009801.
Naylor, P., N. C. Sargent, A. J. Crosbie, A. P. Tilsed, and S. G. Goodyear (1996) Gravity drainage during gas injection, *Pet. Geosci.*, *2*(1), 69–74.
Oak, M. J. (1990), Three-phase relative permeability of water-wet Berea, paper SPE-20183-MS presented at SPE/DOE Enhanced Oil Recovery Symposium, Society of Petroleum Engineers, Tulsa, Okla., 22–25 Apr.
Oak, M. J. (1991), Three-phase relative permeability of intermediate-wet Berea sandstone, paper SPE-22599-MS presented at SPE Annual Technical Conference and Exhibition, Society of Petroleum Engineers, Dallas, Tex., 6–9 Oct.
Oak, M.J., L.E. Baker, and D.C. Thomas (1990), Three-phase relative permeability of Berea sandstone, *J. Pet. Technol., SPE-17370-PA*, doi:10.2118/17370-PA.
Pandy, S., P. A. Forsyth, R. W. Falta, Y. Wu, and P. S. Huyakorn (1995), Considerations for robust compositional simulations of subsurface nonaqueous phase liquid contamination and remediation, *Water Resour. Res.*, *31*(5), 1273–1289.
Parker, J. C., R. J. Lenhard, and T. Kuppusamy (1987), A parametric model for constitutive properties governing multiphase flow in porous media, *Water Resour. Res.*, *23*(4), 618–624.
Pini, R., and S. M. Benson (2013), Simultaneous determination of capillary pressure and relative permeability curves from core-flooding experiments with various fluid pairs, *Water Resour. Res.*, *49*, 3516–3530, doi:10.1002/wrcr.20274.
Piri, M., and M. J. Blunt (2005a), Three-dimensional mixed-wet random pore-scale network modeling of two-and three-phase flow in porous media. I. model description, *Phys. Rev. E*, *71*(2), 026301.
Piri, M., and M. J. Blunt (2005b), Three-dimensional mixed-wet random pore-scale network modeling of two-and three-phase flow in porous media. II. Results, *Phys. Rev. E*, *71*(2), 026302.
Reynolds, C., M. J. Blunt, and S. Krevor (2014), Impact of reservoir conditions on CO_2-Brine relative permeability in sandstones, 12th International Conference on Greenhouse Gas Control Technologies, GHGT-12, *Energy Procedia*, *63*, 5577–5585, doi:10.1016/j.egypro.2014.11.591.
Rezaveisi, M., B. Rostami, R. Kharrat, S. Ayatollahi, and C. Ghotbi (2010), Experimental investigation of tertiary oil gravity drainage in fractured porous media, *Spec. Top. Rev. Porous Media Int. J.*, *1*(2), 179–191, doi:10.1615/SpecialTopicsRevPorousMedia.v1.i2.70.
Sahni, A., J. Burger, and M. J. Blunt (1998), Measurement of three phase relative permeability during gravity drainage using CT, paper SPE-39655-MS presented at SPE/DOE Improved Oil Recovery Symposium, Society of Petroleum Engineers, Tulsa, Okla., 19–22 Apr.
Saraf, D. N., J. P. Batycky, C. H. Jackson, and D. B. Fisher (1982), An experimental investigation of three-phase flow of water-oil-gas mixtures through water-wet sandstones, paper SPE-10761-MS presented at SPE California Regional Meeting, Society of Petroleum Engineers, San Francisco, Calif., 24–26 March.
Sarem, A. M. (1966), Three-phase relative permeability measurements by unsteady-state method, *SPE J.*, *6*(3), 199–205.
Schneider, F. N., and W. W. Owens (1970), Sandstone and carbonate two- and three-phase relative permeability characteristics, *SPE J.*, *249*, 75–84, doi:10.2118/2445-PA.
Shahrokhi, O., S. M. Fatemi, M. Sohrabi, S. Ireland, and K. Ahmed (2014), Assessment of three phase relative permeability and hysteresis models for simulation of water-alternating-gas (WAG) injection in water-wet and mixed-wet systems, paper SPE-169170-MS presented at SPE Improved Oil Recovery Symposium, Society of Petroleum Engineers, Tulsa, Okla., 12–16 Apr.
Shahverdi, H., and M. Sohrabi (2012), Three-phase relative permeability and hystresis model for simulation of water alternating gas (WAG) injection, paper SPE-152218-MS presented at SPE Improved Oil Recovery Symposium, Society of Petroleum Engineers, Tulsa, Okla., 14–18 Apr.
Shahverdi, H., and M. Sohrabi (2013), An improved three-phase relative permeability and hysteresis model for the simulation of a water-alternating-gas injection, *SPE J.*, *18*(5), 841–850, doi:10.2118/152218-PA.
Shahverdi, H., M. Sohrabi, S. M. Fatemi, M. Jamiolahmady, S. Ireland, and G. Rabertson (2011) Evaluation of three-phase relative permeability models for WAG injection using water-wet and mixed-wet core flood experiments, paper SPE-143030-MS presented at SPE EUROPEC/EAGE Annual Conference and Exhibition, Society of Petroleum Engineers, Vienna, Austria, 23–26 May.

Siddiqui, S., P. J. Hicks, and A. S. Grader (1996), Verification of Buckley-Leverett Three-Phase Theory Using Computerized Tomography, *J. Pet. Sci. Eng.*, *15*(1), 1–21, doi:10.1016/0920-4105(95)00056-9.

Skauge, A., and J. A. Larsen (1994), Three-phase relative permeabilities and trapped gas measurements related to WAG processes, paper SCA 9421 presented Proceedings of the International Symposium of the Society of Core Analysts, Stavanger, Norway.

Spiteri, E. J., R. Juanes, M. J. Blunt, and F. M. Orr (2008), A new model of trapping and relative permeability hysteresis for all wettability characteristics, *SPE J.*, *13*(3), 277–288, doi:10.2118/96448-PA.

Stone, H. L. (1970), Probability model for estimating three-phase relative permeability, *J. Pet. Tech.*, *22*(2), 214–218, doi:10.2118/2116-PA.

Stone, H. L. (1973), Estimation of three-phase relative permeability and residual oil data, *PETSOC-73-04-06*, doi:10.2118/73-04-06.

Sun, A. Y., A. Kianinejad, J. Lu, and S. Hovorka (2014), A frequency-domain diagnosis tool for early leakage detection at geologic carbon sequestration sites, 12th International Conference on Greenhouse Gas Control Technologies, GHGT-12, *Energy Procedia*, *63*, 4051–4061, doi:10.1016/j.egypro.2014.11.437.

Vizika, O., and J. M. Lombard (1996), Wettability and spreading: Two key parameters in oil recovery with three-phase gravity drainage, *SPE Reservoir Eng.*, *11*(1), 54–60.

Zhou, D., and M. J. Blunt (1997), Effect of spreading coefficient on the distribution of light non-aqueous phase liquid in the subsurface, *J. Contam. Hydrol.*, *25*(1), 1–19, doi:10.1016/S0169-7722(96)00025-3.

Zuo, L., S. Krevor, R. W. Falta, and S. M. Benson (2012), An experimental study of CO_2 exsolution and relative permeability measurements during CO_2 saturated water depressurization, *Transp. Porous Media*, *91*(2), 459–478, doi:10.1007/s11242-011-9854-2.